

EXTENSION OF RAYLEIGH-TAYLOR INSTABILITY
THEORY WITH APPLICATIONS

Thesis by
Christopher George Whipple

In Partial Fulfillment of the Requirements
for the Degree of
Doctor of Philosophy

California Institute of Technology
Pasadena, California

1974

(Submitted April 29, 1974)

ACKNOWLEDGMENTS

I wish to express my sincere gratitude to Professor Milton Plesset for his advice and suggestions on this research. His most helpful assistance has made my graduate study most enjoyable.

Appreciation for financial assistance is due to the National Science Foundation, the Institute's Graduate Teaching and Research Assistantships programs, the Caltech Fellowship program, and to the Achievement Rewards for College Scientists Foundation, Inc. Acknowledgment is also due to the Office of Naval Research for their support of much of this investigation.

I wish to thank Dr. Howard Winet for conducting many experiments applicable to this research and for his many comments on the biological portions of this work. In addition, I wish to thank David Hofstad for his assistance in much of the experimental work.

Much appreciation is due to Helen Burrus, Barbara Hawk, and Cecilia Lin for their aid and helpful comments on the preparation of this manuscript.

Finally, I wish to thank my wife, Franny, for her help in many areas of my graduate study, particularly in the preparation of this thesis.

ABSTRACT

A theoretical derivation is presented for interfacial waves, both stable and unstable, which includes viscosity and surface tension. This result is extended to the case where one fluid has a finite thickness and is bounded by a rigid boundary or a free surface. As these solutions present formidable algebraic difficulties, approximate forms of solutions, which are motivated by physical arguments, are also given, and, through the use of a computer, the full theoretical result is shown to be fairly accurately reproduced by these approximations. The theory is used to give an explanation of the bioconvection patterns which have been observed with cultures of microorganisms which have negative geotaxis. Since such organisms tend to collect at the surface of a culture and since they are heavier than the culture medium the conditions for Rayleigh-Taylor instability are met. It is shown that the observed patterns are quite accurately explained by the theory. Similar observations with a viscous liquid loaded with small glass spheres are described. A behavior similar to the bioconvective patterns with microorganisms is found and the results are also explained quantitatively by Rayleigh-Taylor instability theory with viscosity. Further physical considerations of the bioconvection demonstrate the validity of the Rayleigh-Taylor instability model, and describe the steady state circulation of microorganisms. An approximate solution to a viscous fluid of finite depth with an exponential density gradient is developed, and the applicability of this result to certain bioconvective situations is discussed.

TABLE OF CONTENTS

CHAPTER		PAGE
I.	INTRODUCTION	1
II.	THEORETICAL SOLUTION TO THE RAYLEIGH-TAYLOR PROBLEM	3
	A. INTRODUCTION AND REVIEW	3
	B. SOLUTION FOR TWO UNBOUNDED FLUIDS	4
	C. THEORETICAL ANALYSIS WITH AN UPPER FLUID OF FINITE THICKNESS	13
	1. Fixed Upper Surface	13
	2. Free Upper Surface	19
III.	APPROXIMATIONS TO THE THEORY	24
	A. INTRODUCTION	24
	B. SMALL DENSITY DIFFERENCE APPROXIMATION	25
	C. ONE-FLUID PROBLEM	31
	D. EQUAL KINEMATIC VISCOSITY APPROXIMATION	35
	E. SUMMARY OF THEORETICAL RESULTS FOR THE LIMITING CASES CONSIDERED	36
IV.	APPROXIMATIONS BASED UPON PHYSICAL ARGUMENTS	39
	A. INTRODUCTION	39
	B. GRAVITATIONAL EFFECTS	39
	C. SURFACE TENSION EFFECTS	40
	D. VISCOUS EFFECTS	43

CHAPTER		PAGE
	E. FINITE UPPER LAYER APPROXIMATIONS	48
V.	COMPARISON WITH OBSERVATIONS	51
	A. INTRODUCTION	51
	B. BIOCONVECTION	51
	C. VISCOUS FLUID CONTAINING GLASS SPHERES	59
VI.	FURTHER COMMENTS ON BIOCONVECTION	62
	A. INTRODUCTION	62
	B. STEADY STATE CIRCULATION	62
	C. EXPONENTIAL DENSITY GRADIENTS	71
VII.	SUMMARY AND CONCLUSIONS	78
	APPENDIX A	79
	APPENDIX B	85
	APPENDIX C	88
	APPENDIX D	90
	APPENDIX E	92
	APPENDIX F	94
	REFERENCES	98
	FIGURES	100

LIST OF FIGURES

FIGURE		PAGE
1	Coordinate system for two unbounded fluids.	4
2	Two fluids beneath the boundary $y = h$.	13
3	Two fluids with free upper surface at $y = h$.	20
4	Growth rate versus wavelength for water accelerated into air.	100
5	Growth rate versus wavelength for glycerol accelerated into air.	101
6	Growth rate versus wavelength for the small density difference case.	102
7	Growth rate versus wavelength for the small density difference case with a free surface at $y = h$.	103
8	Preferred wavelength versus depth for small density difference, free surface case.	104
9	Growth rate versus wavelength for rigid upper boundary.	105
10	Preferred wavelength versus depth for rigid boundary case.	106
11	Side view of <u>Tetrahymena pyriformis</u> culture.	107
12	Top view of <u>Tetrahymena pyriformis</u> culture.	108
13	Top view of glass beads in viscous liquid.	109
14	Nondimensional curve of growth rate versus wave number for exponential density gradient.	110

I. INTRODUCTION

Viscous effects in Rayleigh-Taylor instability have not been considered beyond the analytical aspects of the problem^[1, 2, 3], and yet there are interesting situations for which the role of viscosity is quite decisive for the behavior of the instabilities. The effect of viscosity is masked in the solution of the problem by the algebraic complication of the result. For this reason, three separate approaches to find the effects of viscosity are discussed.

First, in Chapter II, the full theoretical solution is derived. The solution is found for two unbounded fluids, as well as for the cases where the upper fluid has finite depth, with either a rigid boundary or a free surface above the upper fluid. The behavior of the fluid interface as described by these results is, as stated previously, quite complicated and a computer was used to obtain usable results. The second approach, detailed in Chapter III, is that of finding approximations based upon the full theory of Chapter II, for certain special cases. In Chapter IV, a third technique is employed. This method gives approximations to the behavior based on physical arguments rather than on approximations to a more complete theory. These three different methods are compared, and the limitations of the approximation are discussed.

Two experimental cases are discussed in Chapter V, and the experimental results are compared to the theoretical predictions. One experimental case, a bioconvection phenomenon, is described

extensively and Rayleigh-Taylor instability is offered as a model for the process. The use of this model is justified in Chapters V and VI, and additional descriptions of special cases of the bioconvection, steady state circulation and an exponential density gradient situation, are developed in Chapter VI.

II. THEORETICAL SOLUTION

TO THE RAYLEIGH-TAYLOR PROBLEM

A. INTRODUCTION AND REVIEW

The theoretical solution to the Rayleigh-Taylor problem was first presented by Rayleigh^[4]: Rayleigh solved the problem of two unbounded, inviscid, incompressible fluids with no surface tension at the interface. He also solved the problem of a single fluid constrained between two plates. In this example the instability was from an assumed exponential density gradient.

Taylor^[5] resolved Rayleigh's initial problem using a different technique, as well as the problem of a uniform sheet of fluid of finite thickness accelerated by air pressure. Bellman and Pennington^[1] gave a solution to the unbounded two fluid problem with viscosity and surface tension; however, several errors appeared in their paper.

Chandrasekhar^[2] also solved the problem for two unbounded fluids, and while his paper is overly complicated and the results not particularly useful as presented, his solution is correct. He also found the solution to the problem with an exponential density gradient in an inviscid fluid.

Others have approached the problem of superposed fluids considering the stable case. Lamb presented the solutions for two inviscid fluids of finite depth^[6], a single fluid with surface tension acting^[7], and the viscous damping of gravity waves^[3]. Harrison^[8] presented a solution for the stable case of two unbounded viscous fluids, and also a solution for the case of a fluid of finite depth over an infinite fluid. He further considered the free surface case. Harrison's

paper contains a large number of errors. Harrison attempted approximations to his solutions as the full answer is far too complicated to be in any way useful without the use of a computer. His approximations are also incorrect.

Three different problems are presented in this chapter. The first is similar to that considered by Bellman and Pennington, that is, the solution for waves at the unstable interface of two viscous, infinitely deep, incompressible fluids with capillarity. The second and third are for a layer of fluid of finite thickness over an infinitely deep fluid with viscosity acting, and capillarity at the fluid interface. One of these cases is for the upper fluid bounded by a rigid wall, the second for a free upper surface. Surface tension at this surface is also included.

B. SOLUTION FOR TWO UNBOUNDED FLUIDS

This situation is as shown in Fig. 1

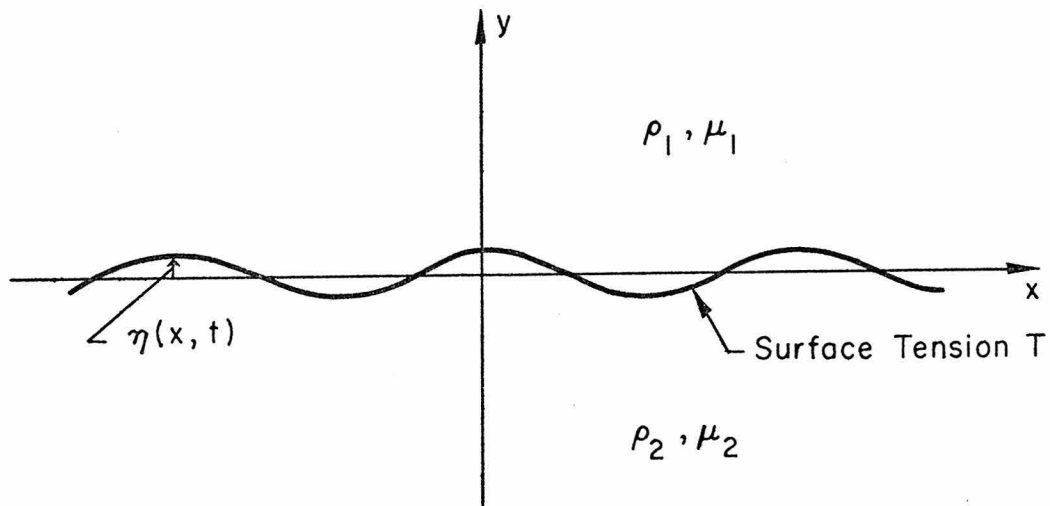


Fig. 1 The fluid interface, η , between two fluids with $\rho_1 > \rho_2$.

To consider the problem in three dimensions adds nothing to the nature of the solution, and serves only to complicate the algebra of the solution. The velocities $u(x, y, t)$ and $v(x, y, t)$ and the pressure $P(x, y, t)$ shall be noted as $u_1, v_1,$ and P_1 for the upper fluid and $u_2, v_2,$ and P_2 for the lower fluid.

The linearized field equations have the same form for both media:

$$\frac{\partial u}{\partial x} + \frac{\partial v}{\partial y} = 0 \quad , \quad (2.1)$$

$$\frac{\partial u}{\partial t} = - \frac{1}{\rho} \frac{\partial P}{\partial x} + \frac{\mu}{\rho} \nabla^2 u \quad , \quad (2.2)$$

and

$$\frac{\partial v}{\partial t} = - \frac{1}{\rho} \frac{\partial P}{\partial y} + \frac{\mu}{\rho} \nabla^2 v - g \quad . \quad (2.3)$$

The negative sign is included in the gravity term, so that $g > 0$. If one wishes to consider the stable case, the substitution of $g < 0$ is the only change that is needed.

Potential and stream functions are introduced such that

$$u = - \frac{\partial \varphi}{\partial x} - \frac{\partial \psi}{\partial y} \quad (2.4)$$

$$v = - \frac{\partial \varphi}{\partial y} + \frac{\partial \psi}{\partial x} \quad (2.5)$$

where a $\varphi_1, \psi_1, \varphi_2,$ and ψ_2 will be used to differentiate the two fluids.

Substitution of Eqs. (2.4) and (2.5) into (2.1) gives

$$\nabla^2 \varphi = 0 \quad . \quad (2.6)$$

Equations (2.4) and (2.5) are also used in Eqs. (2.2) and (2.3) to

give

$$\frac{\partial^2 \varphi}{\partial x \partial t} + \frac{\partial^2 \psi}{\partial y \partial t} = \frac{1}{\rho} \frac{\partial P}{\partial x} + \frac{\mu}{\rho} \nabla^2 \left[\frac{\partial \varphi}{\partial x} + \frac{\partial \psi}{\partial y} \right] , \quad (2.7)$$

and

$$\frac{\partial^2 \varphi}{\partial y \partial t} - \frac{\partial^2 \psi}{\partial x \partial t} = \frac{1}{\rho} \frac{\partial P}{\partial y} + g + \frac{\mu}{\rho} \nabla^2 \left[\frac{\partial \varphi}{\partial y} - \frac{\partial \psi}{\partial x} \right] . \quad (2.8)$$

To remove the pressure terms in these equations, Eq. (2.7) is differentiated with respect to y , (2.8) with respect to x , and one resulting equation is subtracted from the other. It is also noted that (2.6) simplifies (2.7) and (2.8). The result is

$$\frac{\mu}{\rho} \nabla^2 \psi = \frac{\partial \psi}{\partial t} . \quad (2.9)$$

A general solution to (2.6) appropriate to the geometry is

$$\varphi = C_1 f_1(t) e^{-\kappa y} \cos \kappa x + C_2 f_2(t) e^{\kappa y} \cos \kappa x . \quad (2.10)$$

The choice of cosine is arbitrary, and perfectly general as C_1 and C_2 may be complex. The solution to (2.9) is

$$\psi = D_1 e^{-my} e^{nt} \sin \kappa x + D_2 e^{my} e^{nt} \sin \kappa x \quad (2.11)$$

where

$$m = (\kappa^2 + n\rho/\mu)^{\frac{1}{2}} . \quad (2.12)$$

Again, the results are perfectly general as no restrictions have been placed on D_1 , D_2 , n or κ . Substitution of φ and ψ into any of the boundary condition equations demonstrates that $f_1(t)$ and $f_2(t)$ must both be replaced by $\exp(nt)$.

Separating φ and ψ into φ_1, φ_2 and ψ_1, ψ_2 , and applying a condition that the velocities must remain bounded as $y \rightarrow \pm \infty$, one finds that

$$\varphi_1 = Ae^{-\kappa y + nt} \cos \kappa x, \quad (2.13)$$

$$\psi_1 = Be^{-m_1 y + nt} \sin \kappa x, \quad (2.14)$$

$$\varphi_2 = Ce^{\kappa y + nt} \cos \kappa x, \quad (2.15)$$

$$\psi_2 = De^{m_2 y + nt} \sin \kappa x, \quad (2.16)$$

where

$$m_1 = (\kappa^2 + n\rho_1/\mu_1)^{\frac{1}{2}}, \quad (2.17)$$

and

$$m_2 = (\kappa^2 + n\rho_2/\mu_2)^{\frac{1}{2}}. \quad (2.18)$$

The substitution of Eqs. (2.13) through (2.16) into (2.4) and (2.5) gives

$$u_1 = (A\kappa e^{-\kappa y} + Bm_1 e^{-m_1 y})e^{nt} \sin \kappa x, \quad (2.19)$$

$$v_1 = (Ae^{-\kappa y} + Be^{-m_1 y})\kappa e^{nt} \cos \kappa x, \quad (2.20)$$

$$u_2 = (C\kappa e^{\kappa y} - Dm_2 e^{m_2 y})e^{nt} \sin \kappa x, \quad (2.21)$$

$$v_2 = (-Ce^{\kappa y} + De^{m_2 y})\kappa e^{nt} \cos \kappa x. \quad (2.22)$$

The interface of the fluids is designated by $\eta(x, t)$, and it may be found from

$$\frac{\partial \eta}{\partial t} = v \text{ at } y = 0. \quad (2.23)$$

Either v_1 or v_2 may be used here, and v_1 is arbitrarily chosen,

giving

$$\eta(x, t) = \frac{\kappa(A+B)e^{nt}}{n} \cos \kappa x . \quad (2.24)$$

Equations (2.2) and (2.3) reduce to the following form:

$$\frac{\partial P}{\partial x} = \rho \frac{\partial^2 \varphi}{\partial x \partial t} , \quad (2.25)$$

$$\frac{\partial P}{\partial y} = \rho \frac{\partial^2 \varphi}{\partial y \partial t} - g\rho . \quad (2.26)$$

Integrating, one finds

$$P_1 = \rho_1 \frac{\partial \varphi_1}{\partial t} - \rho_1 g y , \quad (2.27)$$

$$P_2 = \rho_2 \frac{\partial \varphi_2}{\partial t} - \rho_2 g y , \quad (2.28)$$

where any constants of integration may, with full generality, be included in the φ -terms.

The boundary conditions at the interface are

$$u_1 = u_2 , \quad (2.29)$$

$$v_1 = v_2 , \quad (2.30)$$

$$\tau_{1yy} + T \frac{\partial^2 \eta}{\partial x^2} = \tau_{2yy} , \quad (2.31)$$

and

$$\tau_{1xy} = \tau_{2xy} , \quad (2.32)$$

where

$$\tau_{1yy} = -P_1 + 2\mu_1 \frac{\partial v_1}{\partial y} , \quad (2.33)$$

$$\tau_{2yy} = -P_2 + 2\mu_2 \frac{\partial v_2}{\partial y} , \quad (2.34)$$

$$\tau_{1xy} = \mu_1 \left(\frac{\partial u_1}{\partial y} + \frac{\partial u_2}{\partial x} \right), \quad (2.35)$$

and

$$\tau_{2xy} = \mu_2 \left(\frac{\partial u_2}{\partial y} + \frac{\partial u_1}{\partial x} \right). \quad (2.36)$$

Because the original equations have been linearized, the terms A, B, C, D, and η are assumed to be small, and any second order product of these terms may be neglected. At the interface $y = \eta$, the terms such as $A \exp(-\kappa y + nt) \cos \kappa x \Big|_{y=\eta}$ may be written as

$$\begin{aligned} A e^{-\kappa \eta} e^{nt} \cos \kappa x &= A e^{nt} (\cos \kappa x) \left(1 - \kappa \eta + \frac{\kappa^2 \eta^2}{2} + \dots \right), \\ &= A e^{nt} \cos \kappa x + O(A\eta). \end{aligned}$$

This result indicates that using $y = 0$ as the interface in the exponential terms is valid as is to be expected.

Substituting Eqs. (2.19) and (2.21) into (2.29), one finds

$$(A\kappa + Bm_1 - C\kappa + Dm_1) e^{nt} \sin \kappa x = 0. \quad (2.37)$$

The use of Eqs. (2.20) and (2.22) in (2.30) gives

$$(A + B + C - D)\kappa e^{nt} \cos \kappa x = 0. \quad (2.38)$$

To evaluate Eq. (2.31), one finds that at the interface

$$\tau_{1yy} = g\rho_1 \eta - \rho_1 A n e^{nt} \cos \kappa x + 2\mu_1 \left[\frac{\partial v_1}{\partial y} \right] \Big|_{y=\eta}, \quad (2.39)$$

$$= \left[g\rho_1 \frac{\kappa(A+B)}{n} - \rho_1 A n + 2\mu_1 (-A\kappa^2 - B\kappa m_1) \right] e^{nt} \cos \kappa x; \quad (2.40)$$

$$\tau_{2yy} = [g\rho_2 \frac{\kappa(A+B)}{n} - \rho_2 Cn + 2\mu_2(-C\kappa^2 + D\kappa m_2)] e^{nt} \cos \kappa x; \quad (2.41)$$

$$T \frac{\partial^2 \eta}{\partial x^2} = - \frac{T\kappa^3(A+B)}{n} e^{nt} \cos \kappa x. \quad (2.42)$$

Equations (2.40), (2.41), (2.42), and (2.31) give

$$A \left[\frac{g(\rho_1 - \rho_2) - T\kappa^3}{n} - \rho_1 n - 2\mu_1 \kappa^2 \right] + B \left[\frac{g(\rho_1 - \rho_2)\kappa - T\kappa^3}{n} - 2\mu_1 \kappa m_1 \right] \\ + C [\rho_2 n + 2\mu_2 \kappa^2] + D [-2\mu_2 \kappa m_2] = 0. \quad (2.43)$$

At the interface, one also finds that

$$\tau_{1xy} = \mu_1 [-2A\kappa^2 - B(\kappa^2 + m_1^2)] e^{nt} \sin \kappa x, \quad (2.44)$$

$$\tau_{2xy} = \mu_2 [2C\kappa^2 - D(m_2^2 + \kappa^2)] e^{nt} \sin \kappa x, \quad (2.45)$$

so that

$$A[2\mu_1 \kappa^2] + B[\mu_1(\kappa^2 + m_1^2)] + C[2\mu_2 \kappa^2] + D[-\mu_2(\kappa^2 + m_2^2)] = 0. \quad (2.46)$$

Equations (2.37), (2.38), (2.43) and (2.46) comprise a set of four linear, homogeneous equations for A, B, C, and D. For a nontrivial solution to exist, the determinant of the coefficients must vanish. If

$$\beta = g\kappa(\rho_1 - \rho_2) - T\kappa^3, \quad (2.47)$$

the determinant is

$$\begin{vmatrix}
 1 & 1 & 1 & -1 \\
 \kappa & m_1 & -\kappa & m_2 \\
 2\mu_1\kappa^2 & \mu_1(\kappa^2+m_1^2) & 2\mu_2\kappa^2 & -\mu_2(m_2^2+\kappa^2) \\
 \frac{\beta}{n} - \rho_1 n - 2\mu_1\kappa^2 & \frac{\beta}{n} - 2\mu_1\kappa m_1 & \rho_2 n + 2\mu_2\kappa^2 & -2\mu_2\kappa m_2
 \end{vmatrix} = 0. \quad (2.48)$$

This determinantal equation is the dispersion relation for $n(\kappa, \rho_1, \rho_2, \mu_1, \mu_2, g)$.

The determinant reduces easily to a three by three determinant

$$\begin{vmatrix}
 m_1 - \kappa & \frac{n}{\kappa} (m_1 - m_2) & m_2 - \kappa \\
 \rho_1 & 2\Delta\mu\kappa + \Delta\rho \frac{n}{\kappa} & -\rho_2 \\
 \rho_1 n + 2\mu_1\kappa(\kappa - m_1) & \frac{\beta}{\kappa} - 2n(\mu_1 m_1 + \mu_2 m_2) & \rho_2 n + 2\mu_2\kappa(\kappa - m_2)
 \end{vmatrix} = 0 \quad (2.49)$$

where $\Delta\rho = \rho_1 - \rho_2$, $\Delta\mu = \mu_1 - \mu_2$.

The expansion of the determinant yields

$$\begin{aligned}
 & n^2 \left[(\Delta\rho)^2 - \frac{(\rho_1 + \rho_2)}{\kappa} (\rho_2 m_1 + \rho_1 m_2) \right] \\
 & + n(2\kappa \Delta\mu) [\Delta\rho(2\kappa - m_1 - m_2) + (\rho_1 + \rho_2)(m_1 - m_2)] \\
 & + \beta/\kappa [\rho_1 m_2 + \rho_2 m_1 - (\rho_1 + \rho_2)\kappa] \\
 & + 4\kappa^2 (\Delta\mu)^2 (\kappa - m_1)(\kappa - m_2) = 0. \quad (2.50)
 \end{aligned}$$

The expansion of the determinant is straightforward, although it involves considerable algebraic detail. The derivation is in Appendix A.

The rationalization of Eq. (2.50) produces a polynomial of tenth degree in n , and gives a number of spurious roots. A more useful approach to obtain the behavior of $n(\kappa)$ is to use a computer with Eq. (2.50), or with the determinant.

In the analysis of the form of $n(\kappa)$, computational solutions show a cutoff wavelength below which the fluids are stable; that is, for κ greater than a certain value, the growth rate, n , has no positive real part. This cutoff is due to the surface tension. If one assumes that no surface tension is present, the growth rate goes to zero as the wave number, κ , becomes infinite (the wavelength, $\lambda = 2\pi/\kappa$, goes to zero). The growth rate exhibits a single maximum, then decreases as the wavelength goes to infinity. The wavelength at which the growth rate is a maximum is the "preferred" wavelength, and should be the wavelength observed in a physical system. The value at which this "preferred" wavelength, λ_m , occurs increases with increasing surface tension and viscosity, and decreases as the relative gravitational force, $g(\rho_1 - \rho_2)/(\rho_1 + \rho_2)$ is increased. The precise dependence of the growth rate upon these quantities is given by (2.50) and is quite complicated. Approximations for special cases can greatly simplify the description of the behavior, and will be presented in a later section.

C. THEORETICAL ANALYSIS WITH AN UPPER FLUID OF FINITE THICKNESS

In the study of bioconvection in microorganism cultures, the measurements indicate that the thickness of the upper layer of fluid is less than that of the observed wavelength. For this reason, the previous solution is presumably not very good in modeling this phenomenon, and the solution in the case of finite thickness of the upper layer should be considered.

There are two different cases: that in which the upper layer is bounded by a fixed upper surface, and that in which the upper surface is free. The solutions may be found by a method similar to the unbounded problem technique.

1. Fixed Upper Surface

The physical situation under consideration is as shown in Fig.

2.

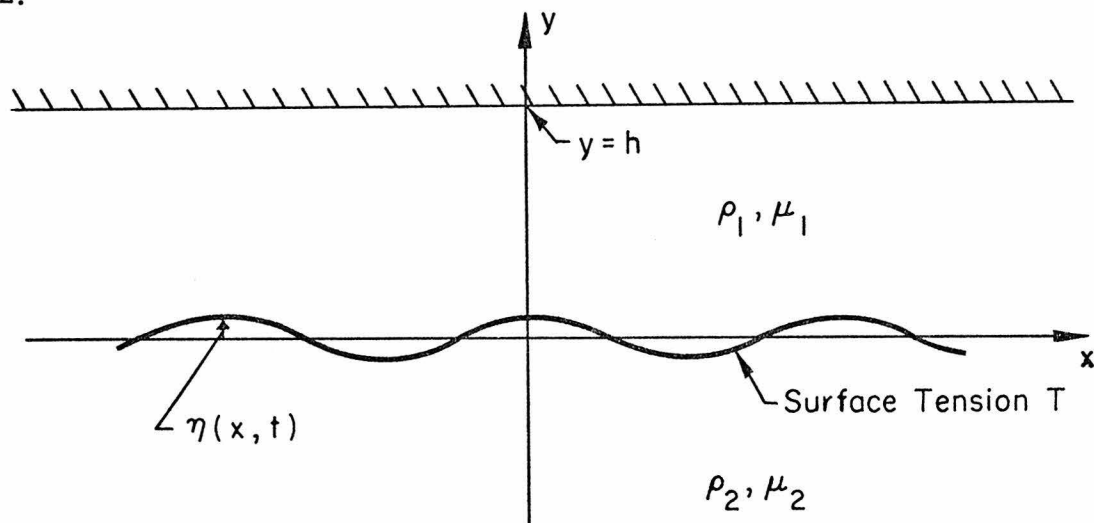


Fig. 2 Two fluids beneath the boundary $y = h$. As before, $\rho_1 > \rho_2$.

The first difference encountered between this problem and the previous problem is that no condition at $y = +\infty$ may be applied.

As a result, the solution is taken to be of the form:

$$\varphi_1 = Ae^{-\kappa y + nt} \cos \kappa x + Be^{\kappa y + nt} \cos \kappa x, \quad (2.51)$$

$$\psi_1 = Ce^{-m_1 y + nt} \sin \kappa x + De^{m_1 y + nt} \sin \kappa x, \quad (2.52)$$

$$\varphi_2 = Ee^{\kappa y + nt} \cos \kappa x, \quad (2.53)$$

$$\psi_2 = Fe^{m_2 y + nt} \sin \kappa x. \quad (2.54)$$

As before,

$$m_1 = (\kappa^2 + n\rho_1/\mu_1)^{\frac{1}{2}}, \quad (2.55)$$

$$m_2 = (\kappa^2 + n\rho_2/\mu_2)^{\frac{1}{2}}, \quad (2.56)$$

and

$$u = -\frac{\partial \varphi}{\partial x} - \frac{\partial \psi}{\partial y}, \quad (2.57)$$

$$v = -\frac{\partial \varphi}{\partial y} + \frac{\partial \psi}{\partial x}. \quad (2.58)$$

The boundary conditions describing the situation at the fluid interface are

$$u_1 = u_2, \quad (2.59)$$

$$v_1 = v_2, \quad (2.60)$$

$$\tau_{1yy} + T \frac{\partial^2 \eta}{\partial x^2} = \tau_{2yy}, \quad (2.61)$$

$$\tau_{1xy} = \tau_{2xy}. \quad (2.62)$$

At the upper surface $y = h$ the boundary conditions are

$$u_1 = 0, \quad (2.63)$$

$$v_1 = 0. \quad (2.64)$$

These two equations provide both a no slip condition and a no penetration condition at the upper boundary.

From Eqs. (2.51) through (2.54), and (2.57) and (2.58) the velocities are

$$u_1 = [A\kappa e^{-\kappa y} + B\kappa e^{\kappa y} + Cm_1 e^{-m_1 y} - Dm_1 e^{m_1 y}] e^{nt} \sin \kappa x, \quad (2.65)$$

$$v_1 = [Ae^{-\kappa y} - Be^{\kappa y} + Ce^{-m_1 y} + De^{m_1 y}] \kappa e^{nt} \cos \kappa x, \quad (2.66)$$

$$u_2 = [E\kappa e^{\kappa y} - Fm_2 e^{m_2 y}] e^{nt} \sin \kappa x, \quad (2.67)$$

$$v_2 = [-Ee^{\kappa y} + Fe^{m_2 y}] \kappa e^{nt} \cos \kappa x. \quad (2.68)$$

As before, the interface η is given by

$$\frac{\partial \eta}{\partial t} = v \Big|_{y=0}. \quad (2.69)$$

For simplicity, v_2 is chosen to be used in (2.69). Integration of this equation yields

$$\eta = \frac{(F-E)}{n} \kappa e^{nt} \cos \kappa x. \quad (2.70)$$

The pressure is the same as it was in the previous solution

$$p_1 = \rho_1 \frac{\partial \phi_1}{\partial t} - g\rho_1 y, \quad (2.71)$$

$$P_2 = \rho_2 \frac{\partial \varphi_2}{\partial t} - g\rho_2 y. \quad (2.72)$$

Substitution of (2.65) and (2.67) into (2.59) gives

$$[A_\kappa + B_\kappa + Cm_1 - Dm_1]e^{nt} \sin \kappa x = [E_\kappa - Fm_2]e^{nt} \sin \kappa x, \quad (2.73)$$

or

$$A_\kappa + B_\kappa + Cm_1 - Dm_1 - E_\kappa + Fm_2 = 0. \quad (2.74)$$

Substitution of (2.66) and (2.68) into (2.60) yields

$$[A - B + C + D]\kappa e^{nt} \cos \kappa x = [-E + F]\kappa e^{nt} \cos \kappa x, \quad (2.75)$$

or

$$A - B + C + D + E - F = 0. \quad (2.76)$$

When the terms in Eq. (2.61) are examined separately, and Eqs. (2.71), (2.72), (2.66), (2.68), (2.51), (2.53), and (2.70) are used, one finds

$$\tau_{1yy} = -P_1 + 2\mu_1 \frac{\partial v_1}{\partial y} \Big|_{y=\eta}, \quad (2.77)$$

$$= g\rho_1 \eta - \rho_1 \frac{\partial \varphi_1}{\partial t} \Big|_{y=0} + 2\mu_1 \frac{\partial v_1}{\partial y} \Big|_{y=0}, \quad (2.78)$$

$$= g\rho_1 \frac{(F-E)}{n} \kappa e^{nt} \cos \kappa x - \rho_1 n A e^{nt} \cos \kappa x - \rho_1 n B e^{nt} \cos \kappa x \quad (2.79)$$

$$+ 2\mu_1 [-A_\kappa - B_\kappa - Cm_1 + Dm_1] \kappa e^{nt} \cos \kappa x,$$

$$= \{A[-\rho_1 n - 2\mu_1 \kappa^2] + B[-\rho_1 n - 2\mu_1 \kappa^2] + C[-2\mu_1 m_1 \kappa] + D[2\mu_1 m_1 \kappa] + E[-g \frac{\rho_1}{n} \kappa] + F[g \frac{\rho_1}{n} \kappa]\} e^{nt} \cos \kappa x. \quad (2.80)$$

$$\tau_{2yy} = -P_2 + 2\mu_2 \frac{\partial v_2}{\partial y} \Big|_{y=\eta}, \quad (2.81)$$

$$= g\rho_2 \eta - \rho_2 \frac{\partial \varphi_2}{\partial t} \Big|_{y=0} + 2\mu_2 \frac{\partial v_2}{\partial y} \Big|_{y=0}, \quad (2.82)$$

$$= g\rho_2 \frac{(F-E)}{n} \kappa e^{nt} \cos \kappa x - \rho_2 n E e^{nt} \cos \kappa x + 2\mu_2 (-E\kappa^2 + m_2 F \kappa) e^{nt} \cos \kappa x, \quad (2.83)$$

$$= \{E[-g \frac{\rho_2}{n} \kappa - \rho_2 n - 2\mu_2 \kappa^2] + F[g \frac{\rho_2}{n} \kappa + 2\mu_2 m_2 \kappa]\} e^{nt} \cos \kappa x. \quad (2.84)$$

$$\Gamma \frac{\partial^2 \eta}{\partial x^2} = \Gamma \kappa^3 \frac{(E-F)}{n} e^{nt} \cos \kappa x, \quad (2.85)$$

$$= \{E[\frac{\Gamma \kappa^3}{n}] - F[\frac{\Gamma \kappa^3}{n}]\} e^{nt} \cos \kappa x. \quad (2.86)$$

Thus, Eq. (2.61) becomes

$$A[\rho_1 n + 2\mu_1 \kappa^2] + B[\rho_1 n + 2\mu_1 \kappa^2] + C[2\mu_1 m_1 \kappa] + D[-2\mu_1 m_1 \kappa] + E[\frac{g\kappa}{n} (\rho_1 - \rho_2) - \frac{\Gamma \kappa^3}{n} - \rho_2 n - 2\mu_2 \kappa^2] + F[-\frac{g\kappa}{n} (\rho_1 - \rho_2) + \frac{\Gamma \kappa^3}{n} + 2\mu_2 m_2 \kappa] = 0. \quad (2.87)$$

Substituting Eqs. (2. 65) through (2. 68) into (2. 62), where

$$\tau_{1xy} = \mu_1 \left(\frac{\partial u_1}{\partial y} + \frac{\partial v_1}{\partial x} \right) \quad (2. 88)$$

and

$$\tau_{2xy} = \mu_2 \left(\frac{\partial u_2}{\partial y} + \frac{\partial v_2}{\partial x} \right), \quad (2. 89)$$

one finds that

$$\begin{aligned} \mu_1 [-A\kappa^2 + B\kappa^2 - Cm_1^2 - Dm_1^2 - A\kappa^2 + B\kappa^2 - C\kappa^2 - D\kappa^2] e^{nt} \sin \kappa x = \\ \mu_2 [E\kappa^2 - Fm_2^2 + E\kappa^2 - F\kappa^2] e^{nt} \sin \kappa x. \end{aligned} \quad (2. 90)$$

This equation reduces to

$$\begin{aligned} A[2\mu_1\kappa^2] + B[-2\mu_1\kappa^2] + C[\mu_1(m_1^2 + \kappa^2)] + D[\mu_1(m_1^2 + \kappa^2)] \\ + E[2\mu_2\kappa^2] + F[-\mu_2(m_2^2 + \kappa^2)] = 0. \end{aligned} \quad (2. 91)$$

For the upper surface boundary conditions, one finds that application of (2. 68) in (2. 63) gives

$$A\kappa e^{-\kappa h} + B\kappa e^{\kappa h} + Cm_1 e^{-m_1 h} - Dm_1 e^{m_1 h} = 0. \quad (2. 92)$$

From Eq. (2. 66) and (2. 64), the remaining boundary condition equation becomes

$$Ae^{-\kappa h} - Be^{\kappa h} + Ce^{-m_1 h} + De^{m_1 h} = 0. \quad (2. 93)$$

Equations (2. 74), (2. 76), (2. 87), (2. 91), (2. 92), and (2. 93) form a six by six determinant which must vanish:

$$\begin{vmatrix}
 e^{-\kappa h} & -e^{\kappa h} & e^{-m_1 h} & e^{m_1 h} & 0 & 0 \\
 \kappa e^{-\kappa h} & \kappa e^{\kappa h} & m_1 e^{-m_1 h} & -m_1 e^{m_1 h} & 0 & 0 \\
 1 & -1 & 1 & 1 & 1 & -1 \\
 \kappa & \kappa & m_1 & -m_1 & -\kappa & m_2 \\
 2\mu_1 \kappa^2 & -2\mu_1 \kappa^2 & \mu_1(m_1^2 + \kappa^2) & \mu_1(m_1^2 + \kappa^2) & 2\mu_2 \kappa^2 & -\mu_2(m_2^2 + \kappa^2) \\
 \rho_1 n + 2\mu_1 \kappa^2 & \rho_1 n + 2\mu_1 \kappa^2 & 2\mu_1 m_1 \kappa & -2\mu_1 m_1 \kappa & \beta/n - \rho_2 n - 2\mu_2 \kappa^2 & -\beta/n + 2\mu_2 m_2 \kappa
 \end{vmatrix} = 0$$

where $\beta = g\kappa(\rho_1 - \rho_2) - T\kappa^3$ as before. (2.94)

No attempts to reduce Eq. (2.94) have been made. Rather, the computer has been used to generate $n(\kappa)$ for specific values of ρ_1 , ρ_2 , μ_1 , μ_2 , T , h and g .

2. Free Upper Surface

The physical situation under consideration is as described by Fig. 3.

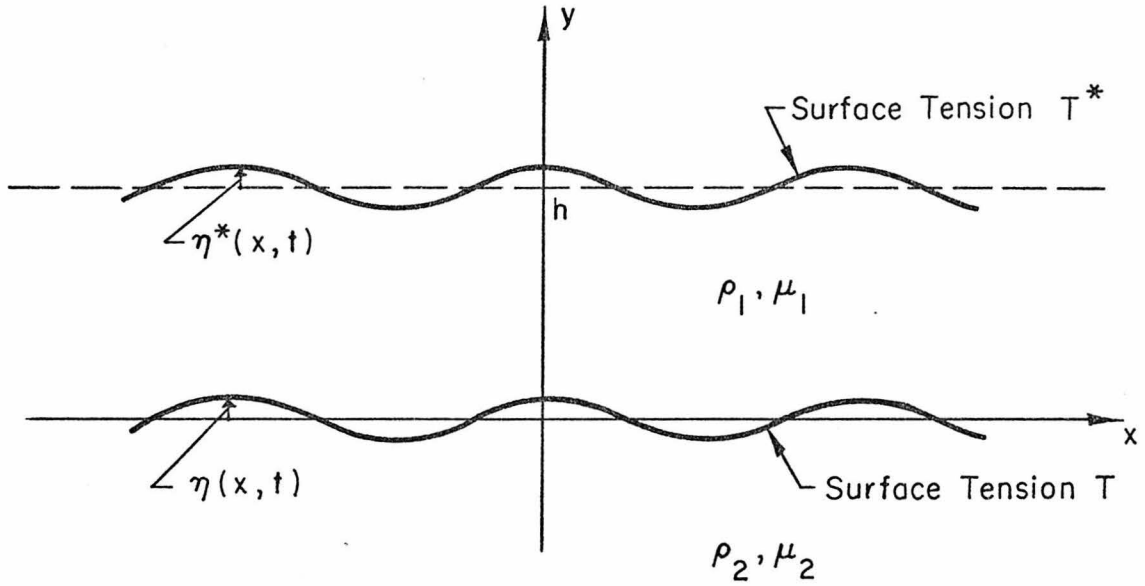


Fig. 3 Two fluids with interface, η , at $y = 0$ and free surface η^* , at $y = h$ where $\rho_1 > \rho_2$.

This case differs from the fixed surface problem in that the two boundary conditions at $y = h$ are

$$\tau_{lxy} = 0, \text{ at } y = \eta^*; \quad (2.95)$$

$$\tau_{lyy} + T^* \frac{\partial^2 \eta^*}{\partial x^2} = 0 \text{ at } y = \eta^*. \quad (2.96)$$

The upper surface, η^* , is found from

$$\frac{\partial \eta^*}{\partial t} = v_1 \Big|_{y=h}. \quad (2.97)$$

Substitution of Eq. (2.66) into (2.97) and integration gives

$$\eta^* = h + (Ae^{-\kappa h} - Be^{\kappa h} + Ce^{-m_1 h} + De^{m_1 h}) \frac{\kappa}{n} e^{nt} \cos \kappa x. \quad (2.98)$$

Equation (2.95) gives

$$\tau_{1xy} = \mu_1 \left(\frac{\partial u_1}{\partial y} + \frac{\partial v_1}{\partial x} \right) \quad (2.99)$$

$$= \mu_1 [-A\kappa^2 e^{-\kappa h} + B\kappa^2 e^{\kappa h} - Cm_1^2 e^{-m_1 h} - Dm_1^2 e^{m_1 h} - A\kappa^2 e^{-\kappa h} \quad (2.100)$$

$$+ B\kappa^2 e^{\kappa h} - C\kappa^2 e^{-m_1 h} - D\kappa^2 e^{m_1 h}] e^{nt} \sin \kappa x = 0.$$

This equation reduces to

$$A[2\kappa^2 e^{-\kappa h}] + B[-2\kappa^2 e^{\kappa h}] + C[(m_1^2 + \kappa^2)e^{-m_1 h}] \quad (2.101)$$

$$+ D[(m_1^2 + \kappa^2)e^{m_1 h}] = 0.$$

Equation (2.96) becomes

$$\tau_{1yy} + T^* \frac{\partial^2 \eta^*}{\partial x^2} = -P_1 + 2\mu_1 \frac{\partial v_1}{\partial y} + T^* \frac{\partial^2 \eta^*}{\partial x^2}, \quad (2.102)$$

$$= \rho_1 g \eta^* - \rho_1 \frac{\partial \varphi_1}{\partial t} + 2\mu_1 \frac{\partial v_1}{\partial y} + T^* \frac{\partial^2 \eta^*}{\partial x^2}. \quad (2.103)$$

This equation will contain the term $\rho_1 gh$, which will be dropped because it is simply the hydrostatic pressure and may be included in φ_1 . Substitution of Eqs. (2.98), (2.51), and (2.66) into (2.103) gives

$$\begin{aligned}
 \tau_{1yy} + T^* \frac{\partial^2 \eta^*}{\partial x^2} &= \rho_1 g [Ae^{-\kappa h} - Be^{\kappa h} + Ce^{-m_1 h} + De^{m_1 h}] \frac{\kappa}{n} e^{nt} \cos \kappa x \\
 &- \rho_1 [nAe^{-\kappa h} + nBe^{\kappa h}] e^{nt} \cos \kappa x + 2\mu_1 [-A\kappa^2 e^{-\kappa h} \\
 &- B\kappa^2 e^{\kappa h} - Cm_1 \kappa e^{-m_1 h} + Dm_1 \kappa e^{m_1 h}] e^{nt} \cos \kappa x \\
 &+ T^* \frac{\kappa^3}{n} [-Ae^{-\kappa h} + Be^{\kappa h} - Ce^{-m_1 h} - De^{m_1 h}] e^{nt} \cos \kappa x.
 \end{aligned}
 \tag{2.104}$$

Simplification of Eq. (2.104) yields

$$\begin{aligned}
 A \left[\frac{\rho_1 g \kappa}{n} - \rho_1 n - 2\mu_1 \kappa^2 - T^* \frac{\kappa^3}{n} \right] e^{-\kappa h} + B \left[\frac{-\rho_1 g h}{n} - \rho_1 n - 2\mu_1 \kappa^2 + T^* \frac{\kappa^3}{n} \right] e^{\kappa h} \\
 + C \left[\frac{\rho_1 g \kappa}{n} - 2\mu_1 m_1 \kappa - T^* \frac{\kappa^3}{n} \right] e^{-m_1 h} + D \left[\frac{\rho_1 g \kappa}{n} + 2\mu_1 m_1 \kappa - T^* \frac{\kappa^3}{n} \right] e^{m_1 h} = 0.
 \end{aligned}
 \tag{2.105}$$

If $\beta = g\kappa(\rho_1 - \rho_2) - T\kappa^3$, and $\alpha = \rho_1 g\kappa - T^* \kappa^3$, the resultant six by six determinant is as follows:

$2\kappa^2 e^{-\kappa h}$	$-2\kappa^2 e^{\kappa h}$	$(m_1^2 + \kappa^2) e^{-m_1 h}$	$(m_1^2 + \kappa^2) e^{2m_1 h}$	0	0
$(\frac{a}{n} - \rho_1 n - 2\mu_1 \kappa^2) e^{-\kappa h}$	$(-\frac{a}{n} - \rho_1 n - 2\mu_1 \kappa^2) e^{\kappa h}$	$(\frac{a}{n} - 2\mu_1 m_1 \kappa) e^{-m_1 h}$	$(\frac{a}{n} + 2\mu_1 m_1 \kappa) e^{m_1 h}$	0	0
1	-1	1	1	1	-1
κ	κ	m_1	$-m_1$	$-\kappa$	m_2
$2\mu_1 \kappa^2$	$-2\mu_1 \kappa^2$	$\mu_1 (m_1^2 + \kappa^2)$	$\mu_1 (m_1^2 + \kappa^2)$	$2\mu_2 \kappa^2$	$-\mu_2 (m_2^2 - \kappa^2)$
$\rho_1 n + 2\mu_1 \kappa^2$	$\rho_1 n + 2\mu_1 \kappa^2$	$2\mu_1 m_1 \kappa$	$-2\mu_1 m_1 \kappa$	$\frac{\beta}{n} - \rho_2 n - 2\mu_2 \kappa^2$	$-\frac{\beta}{n} + 2\mu_2 m_2 \kappa^2$

= 0.

(2.106)

Again, the computer can be used to generate the function $n(\kappa)$, for given values of $T, T^*, \rho_1,$

$\rho_2, \mu_1, \mu_2, h,$ and $g.$

III. APPROXIMATIONS TO THE THEORY

A. INTRODUCTION

Several special cases exist in which approximations to the full theory produce simple, meaningful results. The first such example is for the bioconvection problem. Measurements taken previously^[9] indicate that very small density and viscosity differences occur between one fluid and the other. The normal range of density difference for bioconvective situations is such that $\Delta \rho / (\rho_1 + \rho_2)$ usually lies between 10^{-3} and 10^{-5} . In this case, the surface tension between the two layers is taken to be zero, as both fluids are water, differing only in the concentration of microorganisms.

The second special case is that in which it may be assumed that one fluid has zero density and viscosity. This is the situation for the problem of a liquid such as water or glycerin accelerated into air.

The final special case to be examined occurs in the case of two fluids with the same value for the kinematic viscosity. When this approximation is appropriate, one notes that $m_1 = (\kappa^2 + n\rho_1/\mu_1)^{\frac{1}{2}} = (\kappa^2 + n/\nu_1)^{\frac{1}{2}}$ is the same as $m_2 = (\kappa^2 + n/\nu_2)^{\frac{1}{2}}$. This simplifies the dispersion relation, Eq. (2.50) and the rationalized dispersion relation is reduced from tenth order to fourth order (actually to fifth order, but one root of the equation is zero).

All of these simplifications will be made for the solution for the unbounded media. Corrections for a finite upper layer will be discussed in Chapter IV.

B. SMALL DENSITY DIFFERENCE APPROXIMATION

For the small density difference case, we begin with the complete Eq. (2.50):

$$\begin{aligned}
 & n^2 [(\Delta\rho)^2 - \frac{(\rho_1 + \rho_2)}{\kappa} (\rho_2 m_1 + \rho_1 m_2)] \\
 & + n(2\kappa \Delta\mu) [\Delta\rho (2\kappa - m_1 - m_2) + (\rho_1 + \rho_2)(m_1 - m_2)] \quad (3.1) \\
 & + \beta/\kappa [\rho_1 m_2 + \rho_2 m_1 - (\rho_1 + \rho_2)\kappa] + 4\kappa^2 (\Delta\mu)^2 (\kappa - m_1)(\kappa - m_2) = 0.
 \end{aligned}$$

We drop all terms of order $(\Delta\rho)^2$, $(\Delta\mu)^2$, $\Delta\rho\Delta\mu$, and note that $m_1 - m_2$ is of order $\Delta\rho$, $\Delta\mu$. The equation reduces to

$$n^2 \frac{(\rho_1 + \rho_2)}{\kappa} (\rho_2 m_1 + \rho_1 m_2) - \beta/\kappa (m_1 \rho_2 + m_2 \rho_1 - \kappa(\rho_1 + \rho_2)) = 0. \quad (3.2)$$

At this point the important quantity $\Delta\rho$ is contained in $\beta = g\kappa\Delta\rho - T\kappa^3$. The equation is still valid to first order if at this point we let

$$\rho_1 = \rho_2 = \rho \quad (3.3)$$

$$\mu_1 = \mu_2 = \mu \quad (3.4)$$

$$m_1 = m_2 = m = (\kappa^2 + n/\nu)^{\frac{1}{2}} \quad (3.5)$$

provided that the density difference is retained in β . Equation (3.2) now may be written

$$2n^2 \rho m - \beta(m - \kappa) = 0. \quad (3.6)$$

We now define the quantity σ_o by

$$\sigma_o^2 = \frac{g\kappa\Delta\rho}{(\rho_1 + \rho_2)} - \frac{T\kappa^3}{(\rho_1 + \rho_2)}, \quad (3.7)$$

and then

$$\beta = (\rho_1 + \rho_2)\sigma_o^2 \approx 2\rho\sigma_o^2. \quad (3.8)$$

Substituting Eq. (3.8) into (3.6) one finds

$$m(n^2 - \sigma_o^2) + \kappa\sigma_o^2 = 0. \quad (3.9)$$

The first approximation is now carried to the limit of very short wavelength, that is, κ becomes large and satisfies

$$\frac{\nu\kappa^2}{\sigma_o} \gg 1. \quad (3.10)$$

We also assume that it is valid to write

$$m = (\kappa^2 + n/\nu)^{\frac{1}{2}} = \kappa \left(1 + \frac{n}{2\nu\kappa}\right)^{\frac{1}{2}} \approx \kappa \left(1 + n/2\nu\kappa^2\right). \quad (3.11)$$

The substitution of (3.11) into (3.9) yields

$$n^2 + 2\nu\kappa^2 n - \sigma_o^2 = 0. \quad (3.12)$$

Solving for n , one finds

$$n = -\nu\kappa^2 + [(\nu\kappa^2)^2 + \sigma_o^2]^{\frac{1}{2}} \quad (3.13)$$

$$\approx \nu\kappa^2 \left[-1 + 1 + \sigma_o^2 / (2(\nu\kappa^2)^2) \right] \quad (3.14)$$

$$\approx \frac{\sigma_o^2}{2\nu\kappa^2} = \frac{g\kappa\Delta\rho}{4\rho\nu\kappa^2} - \frac{T\kappa^3}{4\rho\nu\kappa^2} \quad (3.15)$$

In Eq. (3.15), as λ ($\lambda = 2\pi/\kappa$) goes to zero, the term $T\kappa/4\rho\nu$ dominates. This term is negative so that $n < 0$ and the interface is stable. For the biological situation, the surface tension T may be assumed equal to zero. In this case one finds

$$n = \frac{g\Delta\rho\lambda}{8\pi\rho\nu} \quad (3.16)$$

Thus, for very short wavelengths the growth rate increases linearly with the wavelength. If $T = 0$, and Eq. (3.9) is considered, the maximum wavelength may be obtained. If

$$g' = \frac{g\Delta\rho}{\rho_1 + \rho_2}, \quad (3.17)$$

then

$$n = -\nu\kappa^2 + [(\nu\kappa^2)^2 + g'\kappa]^{\frac{1}{2}} \quad (3.18)$$

At the preferred wavelength n has its maximum and $dn/d\kappa = 0$. One finds

$$\frac{dn}{d\kappa} = 0 = -2\nu\kappa + \frac{4\nu^2\kappa^3 + g'}{2(\nu^2\kappa^4 + g'\kappa)^{\frac{1}{2}}} \quad (3.19)$$

which gives the results

$$\kappa_m = \frac{1}{2} \left(\frac{g'}{\nu^2} \right)^{\frac{1}{3}}, \quad (3.20)$$

so that

$$\lambda_m = 4\pi \left(\frac{\nu^2}{g'} \right)^{\frac{1}{3}} \quad (3.21)$$

It should be noted that this approximation is predicated on the assumption that

$$\frac{\nu\kappa^2}{\sigma_0} \gg 1.$$

At $\kappa = \kappa_m$, one finds that

$$\frac{\nu\kappa^2}{\sigma_0} = \frac{1}{(8)^{\frac{1}{2}}} = 0.354 \quad (3.22)$$

and that the assumption of a short wavelength is not valid at the maximum growth rate. While poor justification exists for the use of this result to predict wavelength, comparison with results obtained from the full theory over a wide range of $\Delta\rho$ and ν indicates that this approximation may be extended to the region $\nu\kappa^2/\sigma_0 \approx 1$, as the predicted wavelengths differ by less than ten per cent for most cases.

For the same problem, the approximation appropriate to the long wavelength is algebraically more complicated. The first approximation to Eq. (3.9) produces the result obtained by Rayleigh and by Taylor; that is, the inviscid solution. This result is not surprising since the viscous force decreases rapidly with increasing wavelength like $O(\lambda^{-2})$, while the inertial or gravitational force varies only as $O(\lambda^{-\frac{1}{2}})$. An improvement to the inviscid result, $n = \sigma_0$, can be obtained by assuming

$$n = \sigma_0(1 + \xi) \quad (3.23)$$

where ξ is a nondimensional quantity, small in comparison to 1. Substitution of Eq. (3.23) into (3.9) yields

$$\left(\kappa^2 + \frac{\sigma_0(1+\xi)}{\nu}\right)^{\frac{1}{2}} [\sigma_0^2(1 + 2\xi + \xi^2) - \sigma_0^2] + \kappa\sigma_0^2 = 0. \quad (3.24)$$

Upon simplification this relation becomes

$$\left(\frac{\nu\kappa^2}{\sigma_0} + 1 + \xi\right)^{\frac{1}{2}} (2\xi + \xi^2) + \left(\frac{\nu\kappa^2}{\sigma_0}\right)^{\frac{1}{2}} = 0. \quad (3.25)$$

As this is the long wavelength approximation,

$$\frac{\nu\kappa^2}{\sigma_0} \ll 1. \quad (3.26)$$

The small, nondimensional term, A, is defined by

$$A = \left(\frac{\nu\kappa^2}{\sigma_0}\right)^{\frac{1}{2}}. \quad (3.27)$$

Substitution of (3.27) into (3.25) gives

$$(1 + \xi + A^2)^{\frac{1}{2}} (2\xi + \xi^2) + A = 0. \quad (3.28)$$

Expanding the square root, we have

$$\left(1 + \frac{\xi}{2} + \frac{A^2}{2}\right) (2\xi + \xi^2) + A = 0. \quad (3.29)$$

Rearranging, and dropping terms of order ξ^3 and $A^2\xi^2$, we obtain

$$2\xi^2 + (2 + A^2)\xi + A = 0. \quad (3.30)$$

Solving Eq. (3.30), we find

$$\xi = -\left(\frac{1}{2} + \frac{A^2}{4}\right) \pm \frac{1}{2} (1 - 2A + A^2 + A^4/4)^{\frac{1}{2}} \quad (3.31)$$

$$= -\frac{1}{2} - \frac{A^2}{4} \pm \frac{1}{2} (1 - 2A + A^2)^{\frac{1}{2}} \left(1 + \frac{1}{4} \left(\frac{A^2}{1-A}\right)^2\right)^{\frac{1}{2}} \quad (3.32)$$

$$= -\frac{1}{2} - \frac{A^2}{4} \pm \frac{1}{2} (1 - A) \left[1 + \frac{1}{8} \left(\frac{A^2}{1-A}\right)^2\right]. \quad (3.33)$$

The neglect of the A^4 term gives

$$\xi = -\frac{1}{2} - \frac{A^2}{4} \pm \left(\frac{1}{2} - \frac{A}{2}\right). \quad (3.34)$$

The positive root is chosen to get the root near $n = \sigma_0$, and the result is

$$\xi = -\frac{A}{2} - \frac{A^2}{4}. \quad (3.35)$$

Entering this result in Eq. (3.23), one finds that

$$n = \sigma_0 - \frac{1}{2} (\nu \kappa^2 \sigma_0)^{\frac{1}{2}} - \frac{1}{4} \nu \kappa^2. \quad (3.36)$$

At the maximum growth rate $dn/d\kappa = 0$. To find this maximum, we write Eq. (3.36) in the form

$$n = g'^{\frac{1}{2}} \kappa^{\frac{1}{2}} - \frac{1}{2} \nu^{\frac{1}{2}} g'^{\frac{1}{4}} \kappa^{\frac{5}{4}} - \frac{1}{4} \nu \kappa^2, \quad (3.37)$$

and differentiate to obtain

$$\frac{dn}{d\kappa} = 0 = \frac{1}{2} g'^{\frac{1}{2}} \kappa^{-\frac{1}{2}} - \frac{5}{8} \nu^{\frac{1}{2}} g'^{\frac{1}{4}} \kappa^{\frac{1}{4}} - \frac{1}{2} \nu \kappa. \quad (3.38)$$

We substitute

$$\chi = \kappa^{\frac{1}{4}} \quad (3.39)$$

into (3.38) and find that

$$\chi^6 + 5/4 \nu^{-\frac{1}{2}} g'^{\frac{1}{4}} \chi^3 - \nu^{-1} g'^{\frac{1}{2}} = 0. \quad (3.40)$$

Solving Eq. (3.40) for χ^3 , we find

$$\chi^3 = \frac{\sqrt{89} - 5}{8} \left(\frac{g'}{\nu^2}\right)^{\frac{1}{4}}. \quad (3.41)$$

Equations (3.41) and (3.39) yield

$$\kappa_m = (\chi^3)^{4/3} = \left(\frac{\sqrt{89} - 5}{8}\right)^{4/3} \left(\frac{g'}{\nu^2}\right)^{1/3}, \quad (3.42)$$

or

$$\kappa_m = 0.455 \left(\frac{g'}{\nu^2}\right)^{1/3}. \quad (3.43)$$

This last equation gives

$$\lambda_m = 4.4\pi \left(\frac{\nu^2}{g'}\right)^{1/3}. \quad (3.44)$$

This approximation predicts the preferred wavelength to be about ten per cent longer than the short wavelength approximation.

C. ONE-FLUID PROBLEM

The case of a heavy fluid over air (or accelerated into air) is again drawn from the complete equation, Eq. (2.50):

$$\begin{aligned} & n^2 \left[(\Delta\rho)^2 - \frac{(\rho_1 + \rho_2)}{\kappa} (\rho_2 m_1 + \rho_1 m_2) \right] \\ & + n [2\Delta\mu\kappa] [\Delta\rho(2\kappa - m_1 - m_2) + (\rho_1 + \rho_2)(m_1 - m_2)] \\ & + \beta/\kappa [\rho_1 m_2 + \rho_2 m_1 - (\rho_1 + \rho_2)\kappa] + 4\kappa^2 (\Delta\mu)^2 (\kappa - m_1)(\kappa - m_2) = 0. \end{aligned} \quad (3.45)$$

We take $\rho_1 = \rho$, $\rho_2 = 0$, $\mu_1 = \mu$, $\mu_2 = 0$, and ignore for the moment the quantity ρ_2/μ_2 as found in m_2 . The result is

$$n^2 \left[\rho^2 - \frac{\rho^2 m_2}{\kappa} \right] + 2n \mu \kappa \rho [2\kappa - m_1 - m_2 + m_1 - m_2] \quad (3.46)$$

$$+ \beta/\kappa [\rho m_2 - \rho \kappa] + 4\kappa^2 \mu^2 (\kappa - m_1)(\kappa - m_2) = 0.$$

Rearranging, we have

$$n^2 \left(\frac{\rho}{\kappa} \right)^2 (\kappa - m_2) + 4n \mu \rho \kappa (\kappa - m_2) - \frac{\beta \rho}{\kappa} (\kappa - m_2) + 4\kappa^2 \mu^2 (\kappa - m_1)(\kappa - m_2) = 0. \quad (3.47)$$

Dividing by $(\kappa - m_2)$, one finds

$$n^2 + 4\nu \kappa^2 n - \beta/\rho + 4\nu^2 \kappa^3 (\kappa - m) = 0, \quad (3.48)$$

where

$$m = (\kappa^2 + n\rho/\mu)^{\frac{1}{2}} = m_1. \quad (3.49)$$

As before, we take

$$\sigma_o^2 = g\kappa - \frac{T\kappa^3}{\rho}, \quad \beta/\rho = \sigma_o^2. \quad (3.50)$$

For the long wavelength case $\nu \kappa^2 / \sigma_o \ll 1$. The last term in (3.48) is very small in comparison with β/ρ , as it is of order $(\nu \kappa^2 / \sigma_o)^2$. Upon dropping this term we obtain the long wavelength approximation

$$n^2 + 4\nu \kappa^2 n - \sigma_o^2 = 0, \quad (3.51)$$

or

$$n \approx \sigma_o - 2\nu \kappa^2 + 2 \frac{(\nu \kappa^2)^2}{\sigma_o}. \quad (3.52)$$

The preferred wavelength is easily found from Eq. (3.51), for the case in which surface tension is not important. At this wavelength

$$\frac{dn}{d\kappa} = 0 = -4\nu\kappa + \frac{16\nu^2\kappa^3 + g}{2(4\nu^2\kappa^4 + g\kappa)^{\frac{1}{2}}}. \quad (3.53)$$

The solution of (3.53) is

$$\kappa_m = \frac{1}{2} \left(\frac{g}{4\nu} \right)^{\frac{1}{3}} \quad (3.54)$$

and

$$\lambda_m = 4\pi \left(\frac{4\nu^2}{g} \right)^{\frac{1}{3}}. \quad (3.55)$$

The short wavelength approximation, $\nu\kappa^2/\sigma_0 \gg 1$, also comes from Eq. (3.48). If

$$m = \left(\kappa^2 + \frac{n}{\nu} \right)^{\frac{1}{2}} \approx \kappa \left(1 + \frac{n}{2\nu\kappa} \right), \quad (3.56)$$

then Eq. (3.48) becomes

$$n^2 + 4\nu\kappa^2 n - \sigma_0^2 + 4\nu^2\kappa^3 \left(\kappa - \kappa \left(1 + \frac{n}{2\nu\kappa} \right) \right) = 0. \quad (3.57)$$

Simplification of this result gives the one fluid, short wavelength approximation

$$n^2 + 2\nu\kappa^2 n - \sigma_0^2 = 0. \quad (3.58)$$

This is the same as the short wavelength approximation for the small density difference case, and as before, for $T = 0$,

$$\kappa_m = \frac{1}{2} \left(\frac{g}{\nu} \right)^{\frac{1}{3}}, \quad (3.59)$$

$$\lambda_m = 4\pi \left(\frac{\nu^2}{g}\right)^{\frac{1}{3}}. \quad (3.60)$$

The predicted value of the wavelength differs in these two cases by a factor of $4^{\frac{1}{3}} = 1.59$. By comparison with the complete accurate theory, we find that the short wavelength approximation produces better estimates.

Another approach to the problem is to solve Eq. (3.48) directly. A dispersion relation is obtained that does not require a long or short wavelength limit, rather just the conditions on the density and viscosity described previously. Equation (3.48) may be written

$$n^2 + 4\nu\kappa^2 n - \sigma_o^2 + 4\nu^2 \kappa^4 = 4\nu^2 \kappa^3 m. \quad (3.61)$$

Squaring both sides and rearranging, we have

$$\begin{aligned} n^4 + 8\nu\kappa^2 n^3 + [24\nu^2 \kappa^4 - 2\sigma_o^2]n^2 + [16\nu^3 \kappa^6 - 8\nu\kappa^2 \sigma_o^2]n \\ + [\sigma_o^4 - 8\nu^2 \kappa^4 \sigma_o^2] = 0. \end{aligned} \quad (3.62)$$

If we introduce the nondimensional quantities

$$z = \frac{n}{\nu\kappa} \quad (3.63)$$

and

$$a = \left(\frac{\sigma_o}{\nu\kappa}\right)^2, \quad (3.64)$$

Eq. (3.62) may be written in the dimensionless form

$$z^4 + 8z^3 + [24 - 2a]z^2 + [16 - 8a]z + [a^2 - 8a] = 0. \quad (3.65)$$

This result is valid even for cases with nonzero surface tension. Its usefulness, however, is limited by three factors. First, the term $\alpha(\kappa)$ may assume the same value for two different values of κ . As κ goes to zero or infinity, $\alpha(\kappa)$ goes to infinity. Second, $\alpha(\kappa)$ depends on both g and T so that a simple curve of z against α is not useful. Finally, in squaring Eq. (3.61) spurious roots are generated that are not solutions to the original equation. All roots must be checked by substitution back into Eq. (3.48).

D. EQUAL KINEMATIC VISCOSITY APPROXIMATION

When both fluids have the same kinematic viscosity $\mu_1/\rho_1 = \mu_2/\rho_2 = \nu$, an expansion of the dispersion relation, Eq. (3.1), can be carried out much more easily. The derivation requires only lengthy algebraic manipulation and is found in Appendix B. If we choose

$$\alpha = (\sigma_0 / \nu \kappa^2)^2, \quad (3.66)$$

$$\gamma = \left(\frac{\rho_1 - \rho_2}{\rho_1 + \rho_2} \right), \quad (3.67)$$

and

$$z = \frac{n}{\nu \kappa^2}, \quad (3.68)$$

then Eq. (3.1) may be written as

$$z^4 + z^3 [1 - \gamma^4 + 8\gamma^2] + z^2 [24\gamma^2 - 2\alpha] + z [-2\alpha - 6\gamma^2 \alpha + 16\gamma^2] + [\alpha^2 - 8\alpha\gamma^2] = 0. \quad (3.69)$$

A simple check shows that as $\gamma \rightarrow 1$, the one-fluid problem, Eq. (3.69) is the same as Eq. (3.65).

E. SUMMARY OF THEORETICAL RESULTS FOR THE LIMITING CASES CONSIDERED

1. Two fluids with small density, small viscosity difference:

For the short wavelength approximation one finds

$$n^2 + 2\nu\kappa^2 n - \sigma_o^2 = 0, \quad (3.70)$$

and

$$n \approx \frac{g\kappa \Delta\rho}{4\rho\nu\kappa^2} - \frac{\Gamma\kappa^3}{4\rho\nu\kappa^2}. \quad (3.71)$$

If surface tension is ignored in this approximation,

$$\lambda_m = 4\pi \left(\frac{\nu^2}{g'}\right)^{\frac{1}{3}}. \quad (3.72)$$

The long wavelength approximation gives

$$n = \sigma_o - \frac{1}{2} (\nu\kappa^2 \sigma_o)^{\frac{1}{2}} - \frac{1}{4} \nu\kappa^2, \quad (3.73)$$

which, in the absence of surface tension, gives

$$\lambda_m = 4.4 \pi \left(\frac{\nu}{g'}\right)^{\frac{1}{3}}. \quad (3.74)$$

2. One-fluid problem:

The long wavelength approximation is

$$n^2 + 4\nu\kappa^2 n - \sigma_o^2 = 0, \quad (3.75)$$

or

$$n \approx \sigma_o - 2\nu\kappa^2 + 2 \frac{\nu^2 \kappa^4}{\sigma_o}. \quad (3.76)$$

In the absence of surface tension, the preferred wavelength will be

$$\lambda_m = 4\pi \left(\frac{4\nu^2}{g}\right)^{\frac{1}{3}}. \quad (3.77)$$

The short wavelength approximation is

$$n^2 + 2\nu\kappa^2 n - \sigma_o^2 = 0 \quad (3.78)$$

which, as before, gives

$$\lambda_m = 4\pi \left(\frac{\nu}{g}\right)^{\frac{1}{3}}. \quad (3.79)$$

A general equation, good for all wavelengths, for the one-fluid problem is

$$z^4 + 8z^3 + [24 - 2\alpha]z^2 + [16 - 8\alpha]z + [\alpha^2 - 8\alpha] = 0, \quad (3.80)$$

where

$$z = \frac{n}{\nu\kappa} \quad (3.81)$$

and

$$\alpha = \left(\frac{\sigma_o}{2}\right)^2. \quad (3.82)$$

3. Two fluids of arbitrary density with the same kinematic viscosity:

If we choose

$$\alpha = \left(\frac{\sigma_o}{2}\right)^2, \quad (3.83)$$

$$\gamma = \frac{(\rho_1 - \rho_2)}{(\rho_1 + \rho_2)}, \quad (3.84)$$

and

$$z = \frac{n}{\nu\kappa} z^2, \quad (3.85)$$

Then the dispersion relation is

$$\begin{aligned} z^4 + z^3[1 - \gamma^4 + 8\gamma^2] + z^2[24\gamma^2 - 2\alpha] + z[-2\alpha - 6\gamma^2\alpha + 16\gamma^2] \\ + [\alpha^2 - 8\alpha\gamma^2] = 0. \end{aligned} \quad (3.86)$$

IV. APPROXIMATIONS BASED UPON PHYSICAL ARGUMENTS

A. INTRODUCTION

Simple approximations to the behavior of superposed fluids may be made by means of basic physical arguments, coupled with the well known results for gravity waves as described, for example, by Lamb. The goal of this method is to produce approximate descriptions of the behavior without the lengthy algebraic manipulations of the previous chapter. It is hoped that this approach will produce greater insight into the nature of the motion. As only the solutions to the equations of motion are of interest, the full derivations are in the appendix. This chapter, with some minor differences, has been published previously^[9].

B. GRAVITATIONAL EFFECTS

We first consider the simplest possible situation in which a non-viscous fluid of density ρ when undisturbed occupies the semi-infinite region $y < 0$ and is acted on by gravity with acceleration g . Suppose that this is the one-fluid problem, that is, that the region $y > 0$ is occupied by a fluid of zero density and viscosity. If the surface, η , is disturbed by a plane wave of small amplitude,

$$\eta(x, t; \kappa) = a_{\kappa}(t) \sin \kappa x, \quad (4.1)$$

it is evident that the oscillations are stable and it is also evident that for small amplitudes they must be simple harmonic. This implies that

$$\ddot{a}_{\kappa} + \omega_0^2 a_{\kappa} = 0. \quad (4.2)$$

The angular frequency, ω_0 , can depend only on g and the wave number, $\kappa = 2\pi/\lambda$, where λ is the wavelength. Dimensional considerations suggest that

$$\omega_0 = (g\kappa)^{\frac{1}{2}}, \quad (4.3)$$

which is the correct and familiar result. One cannot be assured by a dimensional argument that the result of Eq. (4.2) should not contain some numerical factor, but the precise result, as given, is derived in Appendix C.

If we now consider the interface between two nonviscous fluids, one of density ρ_1 in the region $y < 0$, subject to the condition $\rho_1 < \rho_2$, then an interfacial wave of small amplitude is stable. It is easy to see that the effective value of gravity for the wave is

$$g' = \frac{\rho_2 - \rho_1}{\rho_2 + \rho_1} g \quad (4.4)$$

since the downward acceleration is changed by the factor $(\rho_2 - \rho_1)/\rho$, and the inertia is also changed, by the factor $(\rho_2 + \rho_1)/\rho$. The small oscillations must again be simple harmonic and the angular frequency will be

$$\omega_0 = (g' \kappa)^{\frac{1}{2}}. \quad (4.5)$$

This again is a well known result, and the derivation is given in Appendix D.

C. SURFACE TENSION EFFECTS

The effect of surface tension on the surface waves may be elucidated in the following way. As before, the gravity field is taken

to act in the $-y$ direction. We suppose that an element of the fluid of density ρ_2 with unit width and cross section dx is elevated to a height η above $y = 0$ into the fluid of density ρ_1 . The downward force on the element due to gravity is then $g(\rho_2 - \rho_1)\eta dx$. The surface tension is given by the product of the surface tension constant, T , and the curvature. This curvature is approximately $\partial^2 \eta / \partial x^2 = -\kappa^2 \eta$, since $\eta = a_\kappa \sin \kappa x$ where a_κ is a small quantity. Thus, the downward force on the element from the surface tension is $T\kappa^2 \eta dx$ and it follows that the net effective acceleration in the $-y$ direction is

$$g'_T = \frac{(\rho_2 - \rho_1)}{(\rho_2 + \rho_1)} g + \frac{T\kappa^2}{(\rho_2 + \rho_1)}. \quad (4.6)$$

The simple harmonic oscillation of $a_\kappa(t)$ is now given by

$$\ddot{a}_\kappa + \omega_o^2 a_\kappa = 0 \quad (4.7)$$

where

$$\omega_o^2 = \kappa g'_T = \frac{(\rho_2 - \rho_1)}{(\rho_2 + \rho_1)} g\kappa + \frac{T\kappa^3}{(\rho_2 + \rho_1)}. \quad (4.8)$$

Equation (4.8) is the well known dispersion formula for an interfacial wave when viscosity is neglected. A more formal derivation of Eq. (4.8) is in Appendix D.

Thus far, ω_o^2 in Eqs. (4.5) and (4.8) has been taken to be a positive quantity since we have assumed $\rho_2 > \rho_1$. There is no mathematical or physical reason that limits the applicability of the discussion to the case in which $\rho_1 > \rho_2$. In place of Eq. (4.7) we would have

$$\ddot{a}_\kappa - \sigma_o^2 a_\kappa = 0 \quad (4.9)$$

where σ_0^2 is a positive quantity,

$$\sigma_0^2 = -\omega_0^2 = \frac{(\rho_1 - \rho_2)}{(\rho_1 + \rho_2)} g\kappa - \frac{T\kappa^3}{(\rho_1 + \rho_2)}. \quad (4.10)$$

As is to be expected, the interfacial wave is now unstable, and the interfacial wave amplitude grows like $\exp(\sigma_0 t)$. This growth phenomenon is the familiar Rayleigh-Taylor instability phenomenon. The description of the instability is, of course, valid only as long as the amplitude remains small, but we must expect that the wavelengths for which σ_0 is largest, as given by the small amplitude theory, will continue to lead in growth beyond the amplitude range for which the small amplitude description is valid.

It is evident from Eq. (4.10) that surface tension can prevent the instability for sufficiently small wavelengths. The limit of instability is given by

$$\kappa_\ell = \left[\frac{(\rho_1 - \rho_2)}{T} g \right]^{\frac{1}{2}}. \quad (4.11)$$

The stability of small hanging water droplets is easily observed and is a familiar effect. This stability is related to the behavior just indicated.

The wave number for which the growth rate is maximized is

$$\kappa_m = \left[\frac{(\rho_1 - \rho_2)}{3T} g \right]^{\frac{1}{2}}. \quad (4.12)$$

D. VISCOUS EFFECTS

Of greater interest here is the action of viscosity upon Rayleigh-Taylor instability. To simplify the physical discussion, we shall drop the term arising from surface tension in the following; its effects can always be included in the way that has just been described. We shall now attempt to develop a simple approach to the damping of stable or unstable interfacial waves. If we consider first the stable case, $\rho_2 > \rho_1$, we describe this in terms of a simple harmonic oscillation,

$$\ddot{a}_k + \omega_o^2 a_k = 0$$

with

$$\omega_o^2 = \frac{(\rho_2 - \rho_1)}{(\rho_1 + \rho_1)} gk.$$

The effect of viscosity clearly will give some damping to these oscillations, and the damping may be easily estimated for some particular cases. First, we consider a heavy fluid (e. g. water, glycerol) in contact with a fluid of negligible dynamic effect (e. g. air) so that we have only to consider a single fluid. If μ is the dynamic viscosity of this fluid, and $\nu = \mu/\rho$ is its kinematic viscosity, then from dimensional considerations the damping of the oscillations should depend only on νk^2 . From the familiar expression for a damped simple harmonic oscillator, the damped surface wave will, in an approximate sense, satisfy an equation of the form

$$\ddot{a}_k + f\nu k^2 \dot{a}_k + \omega_o^2 a_k = 0. \tag{4.13}$$

The factor f is, of course, unknown, and actually the exact description of damped surface waves cannot be accurately described in such simple terms except in limiting situations. As is derived in Appendix E, it is well known^[7] that, for very small damping, surface wave oscillations have the form

$$e^{i\omega_o t} e^{-2\nu\kappa^2 t}$$

and this form would be obtained from Eq. (4.13) with $f = 4$:

$$\ddot{a}_\kappa + 4\nu\kappa^2 \dot{a}_\kappa + \omega_o^2 a_\kappa = 0 \quad \nu\kappa^2 \ll \omega_o \quad (4.14)$$

as may be seen by writing

$$a_\kappa(t) = a_\kappa(o) e^{nt} \quad (4.15)$$

so that for n , the equation becomes

$$n^2 + 4\nu\kappa^2 n + \omega_o^2 = 0, \quad \nu\kappa^2 \ll \omega_o. \quad (4.16)$$

Equations (4.14) and (4.16) then describe the long wavelength limit in which damping is very small. Of more interest is the case in which viscous damping is important. Some guidance in that direction may be obtained from the already known behavior in the "creeping motion" limit for which

$$n \approx \frac{-\omega_o^2}{2\nu\kappa^2} \quad (4.17)$$

This result is also derived in Appendix E. The relation Eq. (4.17) suggests that the short wavelength limit, or the limit in which damping is important, may be described by

$$\ddot{a}_\kappa + 2\nu\kappa^2 \dot{a}_\kappa + \omega_0^2 a_\kappa = 0 \quad \nu\kappa^2 \gg \omega_0 \quad (4.18)$$

or by

$$n^2 + 2\nu\kappa^2 n + \omega_0^2 = 0 \quad \nu\kappa^2 \gg \omega_0. \quad (4.19)$$

For the unstable case we would then have

$$n^2 + 4\nu\kappa^2 n - \sigma_0^2 = 0 \quad \nu\kappa^2 \ll \sigma_0 \quad (4.20)$$

and

$$n^2 + 2\nu\kappa^2 n - \sigma_0^2 = 0 \quad \nu\kappa^2 \gg \sigma_0. \quad (4.21)$$

We should expect that Eq. (4.21) would be of particular interest since it covers the range in which viscous damping is important. We shall use Eq. (4.21) over the whole range of κ even though it may not be accurately permissible when $\nu\kappa^2 \sim \sigma_0$. In direct comparison with values calculated from the full theory over a wide range of density differences, viscosities, and surface tensions, the short wavelength approximation has been found to be better than the long wavelength approximation in two respects. First, the wavelength at which the growth rate is maximized as predicted by the accurate theory is found to be closer to the short wavelength approximation of this preferred wavelength than with that obtained by the long wavelength approximation. This value, as predicted by the short wavelength approximation is

$$\lambda_m = 4\pi \left(\frac{\nu}{g'} \right)^{\frac{2}{3}}. \quad (4.22)$$

The second reason that the short wavelength approximation is considered better than the long wavelength approximation is that the values of the growth rate computed from the short wavelength approximation are closer to those of the full theory than the values computed from the long wavelength approximation.

The great advantage of the simple model which leads to Eq. (4.21) is that it gives a direct physical insight to an expectation of a maximum in $n(\kappa)$, a maximum which must occur in the unstable physical situation. The disturbance with the wavelength at which this maximum occurs grows more rapidly than any other. It is true that the theory is limited to small disturbances, but the disturbance which grows most rapidly should continue to be the leading one into the range where amplitudes are large.

Curves $n(\lambda)$ have been generated for several different instability situations, by the full theory of Chapter II, and the approximations of Chapters III and IV. The first such case is that of water accelerated into air with net acceleration $2g$. The density and dynamic viscosity of the air were set equal to zero, but the interfacial surface tension has been included. Computations made for this situation by the short wavelength approximation, the long wavelength approximation, and the full theory agree to four or five significant digits. This close agreement, however, cannot be taken as justification of either approximate theory as surface tension, not viscosity, gives the significant modification of the gravitational effect. This result is shown in Fig. 4. Figure 5 shows the approximate $n(\lambda)$ computed from Eq. (4.21) (the short

wavelength approximation) as well as the results obtained from computation of the full theory of Chapter II for glycerin accelerated into air with acceleration $2g$. Surface tension was included in this computation, but computations without the surface tension term give only slightly different results. For this example, the viscosity is the decisive quantity. Agreement is seen to be quite satisfactory.

A second example which will be considered is the case of two fluids in which the density difference is small. Further, it will be supposed that the two fluids have the same kinematic viscosity and that no surface tension acts at the interface, as would be the case of two superposed, miscible fluids. In the short wavelength limit, that is, in the limit in which viscosity is important, we again use the damped oscillator equation in the form

$$n^2 + 2\nu\kappa^2 n + \omega_0^2 = 0, \quad \nu\kappa^2 \gg \omega_0, \quad (4.23)$$

for the stable case, and

$$n^2 + 2\nu\kappa^2 n - \sigma_0^2 = 0, \quad \nu\kappa^2 \gg \sigma_0, \quad (4.24)$$

for the unstable case. The unstable case is of greater interest, and as before, the maximum value of n occurs for a wavelength

$$\lambda_m = 4\pi (\nu^2/g')^{\frac{1}{3}}$$

where

$$g' = g \frac{\Delta \rho}{\rho_1 + \rho_2} .$$

A formal justification of Eq. (4.24) is provided in the previous chapter. A comparison of the approximate solution and the exact solution shows that the approximate formulation is quite accurate (see Fig. 6). Equations (4.23) and (4.24) describe a wave on the interface of two fluids where $\rho_1 = \rho_2 + \Delta\rho$ and $\mu_1 = \mu_2 + \Delta\mu$ where $\Delta\rho$ and $\Delta\mu$ are both small compared with ρ and μ , respectively.

E. FINITE UPPER LAYER APPROXIMATIONS

In the limiting cases of small density difference and very large density difference, the short wavelength approximations are the same:

$$n^2 + 2\nu\kappa^2 n - \sigma_o^2 = 0, \quad (4.25)$$

with

$$\sigma_o^2 = \frac{g\kappa(\rho_1 - \rho_2)}{(\rho_1 + \rho_2)} - \frac{T\kappa^3}{(\rho_1 + \rho_2)}. \quad (4.26)$$

It is known [6] that for two inviscid fluids, one of finite thickness bounded by a rigid wall, the behavior is described by

$$n^2 = \frac{g\kappa(\rho_1 - \rho_2) - T\kappa^3}{\rho_1 \coth \kappa h + \rho_2} \quad (4.27)$$

where h is the thickness of the upper layer.

For a free upper surface over a layer of fluid of finite thickness as described in Chapter III, the known [6] result is

$$n^2 = \frac{g\kappa(\rho_1 - \rho_2) - T\kappa^3}{\rho_1 + \rho_2 \coth \kappa h}. \quad (4.28)$$

where T refers to the surface tension at the fluid interface.

Through these two solutions an improvement may be made to the short wavelength approximation for those situations where the depth of the upper fluid cannot be considered infinite.

For the fixed upper surface one takes

$$n^2 + 2\nu\kappa^2 n - \frac{g\kappa(\rho_1 - \rho_2) - T\kappa^3}{\rho_1 \coth \kappa h + \rho_2} = 0, \quad (4.29)$$

and for the free surface

$$n^2 + 2\nu\kappa^2 n - \frac{g\kappa(\rho_1 - \rho_2) - T\kappa^3}{\rho_1 + \rho_2 \coth \kappa h} = 0. \quad (4.30)$$

In comparison with the computer-generated curves from the six by six determinants, these approximations are relatively good until the upper fluid depth becomes quite small ($h/\lambda < 0.1$). As the depth of the upper layer decreases, the approximations do significantly improve the short wavelength approximations for an unbounded fluid. The derivations of Eqs. (4.27) and (4.28) are in Appendix F.

The $n(\lambda)$ predicted by the approximate theory for the finite upper layer problem do not correlate to those generated from the full theory as accurately as was the case for unbounded fluids. This discrepancy is not surprising since some of the important boundary conditions at the upper surface are ignored. Specifically, the no-slip condition imposed on the fixed surface for the exact theory is not applied in the approximation. Similarly, the requirement that the viscous shear stress vanish at the free surface is not applied in the free surface approximation. One would expect to find wider disparities between the two methods as the upper fluid depth is decreased, and this

does occur. Figure 7 shows curves generated by both the approximate method just described, and by computation from the six by six determinant, as described in Chapter II, for two fluids of small density difference with an upper fluid depth of 0.15 cm with the free surface boundary. The variation of predicted wavelength with upper fluid depth for this free surface case is shown in Fig. 8. For the fixed upper surface Fig. 9 shows $n(\lambda)$ computed from the exact theory with depth of 0.2 cm, $\rho_1 = 1.4 \text{ gm/cm}^3$, $\rho_2 = 0.943 \text{ gm/cm}^3$, and $\mu_1 = \mu_2 = 9.43 \text{ poise}$. The results from the approximate method are not included because at this depth the disparity is too great. Figure 10 gives curves of λ_m as a function of h for the fixed surface with density and viscosity as described for Fig. 9.

V. COMPARISON WITH OBSERVATIONS

A. INTRODUCTION

It is desirable to compare the theoretical solution to the Rayleigh-Taylor problem with experimental observations. The first experimental work directed at this problem was performed by Lewis^[10] but his experiments are not suited toward determining viscous effects. Further experimental work has been carried out by Emmons, Chang, and Watson^[11]. This work deals with surface tension effects and viscosity is ignored. Similarly, an inviscid situation was investigated by Cole and Tankin^[12].

Observations have been made of instabilities in microorganism cultures dating back a hundred years, but this instability was not recognized as being of the Rayleigh-Taylor type until very recently^[9, 13]. This phenomenon will be discussed in detail in this chapter. To complement the observations of microorganism cultures, experiments were performed with a very viscous liquid (Dow-Corning DC-200; $\nu = 10$ Stokes) containing a layer of glass spheres. Convection patterns similar to those in the biological fluid were observed. These experiments will also be discussed later in the chapter.

B. BIOCONVECTION

It has long been known that certain microorganisms (ciliates and flagellates) exhibit negative geotaxis, that is, they swim upward in their fluid medium even though they are more dense than the surrounding fluid. When a sufficiently dense layer has formed at the top, a bioconvective pattern develops. Characteristic of these patterns are

fingers falling from the top layer into the lower liquid. Further, these fingers are separated in a rather regular pattern (see Figs. 11 and 12).

Many attempts have been made to provide an explanation of how these bioconvective patterns form. Thermal instability was offered as an explanation because the patterns that develop resemble Bénard cells. However, in an experiment performed by R. Donnelly in which a culture dish of Tetrahymena pyriformis was placed on ice, the patterns were still observed in spite of the stabilizing thermal gradient^[14].

Three other possible explanations for the bioconvective patterns include (i) directed motion of individuals due to the exhaustion of oxygen or nutrients in the center of the nodes, or fingers; (ii) viscous attachment of individuals; (iii) reduction of swimming on collision. All three arguments may be rejected on the grounds that such effects could not produce patterns in a chemically inert liquid containing glass spheres. Further, the second and third may also be rejected because there is no evidence for them under the microscope, and because cultures washed in pure water (with any high viscosity filaments presumably removed) still exhibit the same patterns^[14]. Finally, an explanation was proposed^[15] based upon perturbations in the uniform density of the upper layer. It is assumed that a region of higher density than average will fall faster, and that the surrounding fluid would be entrained, creating the finger-like patterns. This explanation is also unacceptable for two reasons. First, measurements taken from a Tetrahymena pyriformis culture^[15] find a maximum density perturbation of 0.6 %, so little reason exists for thinking that the more dense regions would fall much faster than the surrounding regions. Second, this explanation

offers no reason to expect that the clusters (fingers) would be a uniform distance apart, and that this distance could be measured and reproduced with the high degree of repeatability that has, in fact, been found.

To show that Rayleigh-Taylor instability is the process by which the bioconvective patterns are formed, the distance between clusters in the falling patterns must be correlated with the predicted wavelength of the theoretical model. In addition to requiring this correlation, we must also provide justification for the use of a continuum model in dealing with the upper layer of fluid.

A full description of the motion of a culture of T. pyriformis follows. Tetrahymena pyriformis is a ciliate, about 5×10^{-3} cm long, which swims with a speed U of about 4.5×10^{-2} cm/sec. If the culture starts with a uniform concentration of cells, C_0 , the cells swim in a manner to produce a net upward drift of cells. Because the cells do not all swim directly upward, one may assume a net upward speed of αU for each cell, where α is a constant computed to be approximately $2/3$. A discussion of this computation appears in the section dealing with the steady state circulation. The density of a T. pyriformis cell is 1.076 gm/cm^3 , and the medium in which it lives is water, with some nutrient additives. Observations by Winet^[13] indicate that upon reaching the surface, 17% of the cells stay in a clearly defined layer on the surface; a layer between 0.1 and 0.6 cm thick. This thickness we designate h . The remaining 83% of the cells reflect from the surface, or from other cells, and swim downward for a distance many times that of the upper layer thickness h . It seems that a considerable amount of time is involved before a cell can turn around and begin

another ascent. From this, one can see that the upper layer concentration, C_u , grows linearly in time, provided that the thickness remains constant. This thickness does remain constant, and its value depends only upon the initial concentration C_o , and on the age of the culture, measured over a much longer time scale than the time of pattern formation. When a certain C_u is reached, patterns begin to develop on the surface (see Fig. 12) resembling individual clusters of high cell concentration separated by regions of lower concentration. At the center of these clusters a node begins to descend. These falling nodes reach velocities of approximately 0.1 cm/sec. This velocity is reached before the nodes have travelled a significant distance, on the order of 0.1 cm, and it is interesting to note that these fall velocities are over twice the swimming velocity of a Tetrahymena pyriformis, and much greater than the Stokes fall speed for a cell falling under the force of gravity (computed to be 6.6×10^{-3} cm/sec). This last statement indicates that the patterns must depend on a cooperative nature of the cells since individual cells could not produce so great a speed.

When a T. pyriformis is moving with constant velocity, there can be no net force acting on it. The self-propulsion of the cell balances both the viscous drag and the gravitational force. The gravitational force on one cell is $V_T \rho_T g$, where V_T is the volume of one T. pyriformis, ρ_T the density, and g the acceleration due to gravity. This gravitational force is partially balanced by a bouyancy force $V_T \rho_o g$, where ρ_o is the density of the medium. For the cell to be nonaccelerating, it must therefore exert a net downward force on the

fluid of $V_T(\rho_T - \rho_o)g$, or $V_T\Delta\rho_Tg$. This is the only significant effect the cell has on the fluid, and results in a net density increase of the fluid. To prove this, we must consider other possible effects that could be caused by the cells.

The first such effect considered is that of the acceleration of the cells. To obtain an estimate of the ratio of the accelerative force to that of the gravitational force, we consider the worst case, that of one cell accelerating from rest. This is the worst case because in fact, all of the cells would never accelerate in the same direction, and their effects on the fluid would cancel (except when the cells reach the surface and stop). The force on a cell due to its own acceleration is $\rho_T V_T U/t$, where t is the time required to reach speed U from rest. The swim speed, U , is approximately ten body lengths per second and is reached in approximately one body length. If we assume that the velocity grows linearly in time from zero to U , then the acceleration time is approximately 0.2 sec. Thus, for the ratio of accelerative force, f_a , to gravitational force, f_g , we have

$$\frac{f_a}{f_g} = \frac{\rho_T V_T U}{t V_T \Delta \rho_T g} = \left(\frac{\rho_T}{\Delta \rho_T} \right) \left(\frac{U}{tg} \right). \quad (5.1)$$

As stated previously, $\Delta\rho_T = 0.076$, $\rho_T = 1.076$, $U = 4.5 \times 10^{-2}$, $t = 0.2$ and $g = 10^3$, all in cgs units. One finds from Eq. (5.1) that

$$\frac{f_a}{f_g} = 3.2 \times 10^{-3}. \quad (5.2)$$

Thus the acceleration forces are quite small in comparison to those of gravity, especially when one notes that this is such an extreme case. Deacceleration occurring when a cell reaches the surface is through the process of an added external force. When a cell reaches the surface, it pushes water above the mean surface level, and gravitational force stops the cell. Surface tension could also act in this case.

The second force that the cells could produce on the fluid, in addition to the gravitational force, is that due to a net momentum flux into the upper layer. If we consider one square centimeter of the upper layer, with thickness h , over an infinite lower fluid with cell concentration C_L , we find that the net upward migration of cells in the lower fluid is with velocity aU . The upward momentum of cells in the lower fluid per unit volume is then $C_L \rho_T V_T aU$. The net horizontal momentum per unit volume is zero. When these cells reach the upper layer, 17% are trapped in the upper layer and the remaining 83% bounce off. If one assumes that the cells that do not stay in the upper layer bounce off such that their net velocity is now aU directed downward, then the net force per unit volume transmitted to one cm^2 of the upper layer is $C_L \rho_T V_T aU(0.17 + 2 \times 0.83)(aU/h)$. This is because aU/h is the rate at which the upper layer receives force/unit volume due to the rising cells. The ratio of the momentum caused force per unit volume, F_m , to that of the gravitational force per unit volume, F_g , is

$$\frac{F_m}{F_g} = \frac{1.83 C_L \rho_T V_T a^2 U^2}{h C_u \Delta \rho_T V_T g}, \quad (5.3)$$

which can be written as

$$\frac{F_m}{F_g} = 1.83 \left(\frac{C_L}{C_u} \right) \left(\frac{\rho_T}{\Delta \rho_T} \right) \left(\frac{a^2 U^2}{hg} \right). \quad (5.4)$$

We know that $C_L/C_u < 1$, $\rho_T/\Delta \rho_T < 15$, $aU = 3 \times 10^{-2}$ cm/sec, $h \geq 0.1$ cm, and that $g \approx 10^3$ cm/sec². Therefore, the estimate of the ratio is

$$\frac{F_m}{F_g} < 2.5 \times 10^{-4}. \quad (5.5)$$

This effect is also negligible.

The minimum concentration observed in the upper layer that will produce bioconvection is 4×10^4 cells/cm³. If one assumes a uniform distribution, the distance between the centers of nearest cells is 3×10^{-2} cm. As the minimum observed value of the wavelength is about 0.5 cm, the effects of individual cells can be ignored. Even for the minimum observed upper layer concentration, in the thinnest observed layer, 0.1 cm, 4000 cells still occupy one square centimeter of the layer. The only significant effect of the cells on the fluid is gravitational, and this results simply in a density increase of the upper layer. The density is $\rho_u = \rho_w + C_u \Delta \rho_T V_T$, where ρ_u is the effective density of the upper layer. Any effects arising from individual cell motions must be of very short wavelength, comparable to the nearest neighbor distance, and are unnoticeable with respect to the large scale phenomenon.

The theoretical solution assumes a step density jump at the fluid interface. While this condition cannot be exactly satisfied for the bio-convective problem, photographs with collimated light taken from the side of a T. pyriformis culture indicate that the concentration change occurs through a thickness always less than 0.1 cm, and usually less than 0.05 cm. It should be pointed out that this distance is only about twice that of the nearest neighbor distance calculated previously, but for most experimental cases the upper layer concentration is over one order of magnitude larger than the concentration used to compute this neighbor distance, so measurements down to 0.05 cm are somewhat meaningful. The lower concentration discussed previously is the worst case and was used for the continuity arguments. In the cases when the thickness of the upper layer is only 0.1 to 0.15 cm, some error is introduced by the assumption of a step density change. When the upper layer is thicker, 0.5 to 0.6 cm, this region of concentration change is less important.

The appropriate theoretical model of these experiments is the solution for two fluids, the upper of finite thickness bounded by a free surface. No surface tension is assumed to act at the fluid interface because the fluids are completely miscible. Surface tension can be included at the free upper surface, but this term produces no significant change over the case where no surface tension is included.

A typical measurement^[15] gives a measured value of $\Delta \rho = 1.21 \times 10^{-4}$, where $\Delta \rho$ here refers to the upper layer density minus the lower layer density. The upper layer in this experiment has a thickness of 0.15 cm, and the observed distance between falling fingers is 1.0 cm. The appropriate approximate equation is

$$n^2 + 2\nu\kappa^2 n - \frac{g\kappa(\rho_1 - \rho_2)}{\rho_1 + \rho_2 \coth(\kappa h)} = 0, \quad (5.6)$$

which is Eq. (4.30). Computations with Eq. (5.6) show that the growth rate, n , will be a maximum at a wavelength of 1.05 cm. This is in excellent agreement with the experimental results. When the appropriate exact theory is applied, a computation gives a preferred wavelength of 0.80 cm for this case. This predicted result is also in fairly good agreement with the experimental result. Figures 7 and 8 show the curves generated by both theoretical methods.

A second experiment, also by Winet, gave the following results. The measured density difference between layers is $\Delta\rho = 9 \times 10^{-3}$ gm/cm³, the thickness of the upper layer is 0.13 cm, although this figure may be inaccurate for reasons previously discussed. The observed distance between fingers is 0.655 cm. The exact theory predicts a preferred wavelength of 0.525 cm for this case. If the upper layer thickness is 0.18 cm, 0.05 cm thicker than measured, and within the range of experimental error for this difficult measurement, the theory predicts a wavelength of 0.60 cm. Again, we have fairly good agreement between the experimental and theoretical results. The approximate theory discussed in Chapter IV predicts a wavelength of 0.65 cm.

C. VISCOUS FLUID CONTAINING GLASS SPHERES

To test the accuracy of the theory, experimental verification was sought over a wide range of density differences and viscosities.

The previously described experiment has very low values of $\Delta \rho$ and μ ($\Delta \rho \sim 0(10^{-4})$ to (10^{-3}) , $\mu = 10^{-2}$). Because of this, an experiment of a somewhat different kind has been performed in which a very viscous liquid (Dow-Corning DC-200, $\nu = 10.$) was loaded with solid glass spherical particles with radii of approximately 0.01 cm. When such a mixture is put in a chamber with a flat top and bottom, the glass spheres will settle on the bottom surface and a fairly uniform layer can be obtained. With a liquid of such high viscosity, the container can be inverted without unwanted circulatory flows. The effective density and thickness of the heavier layer can be determined before the chamber is inverted, and separate experiments can give the viscosity of the fluid containing the glass particles. A typical value for the density of the loaded liquid is $\rho_1 = 1.4 \text{ gm/cm}^3$ and the density of the unloaded DC 200 is $\rho = 0.943 \text{ gm/cm}^3$. The observed instability pattern is shown in Fig. 13. The observed thickness of the upper layer is $h = 0.20 \text{ cm}$. The observed distance between the fingers is 0.8 cm. The appropriate theoretical model for this case is the solution for finite upper layer thickness bounded by a rigid boundary. For reasons explained in Chapter IV, the approximate method does not give very good results for values of h this small (see Fig. 10). The appropriate curve from the full theory is shown in Fig. 9. This predicts a wavelength of 0.7 cm which is in close agreement with the experimental value. For this experiment, the concentration of glass particles was found to be $7.3 \times 10^4/\text{cm}^3$, which predicts that the distance between the centers of neighboring particles is $2.4 \times 10^{-2} \text{ cm}$, a term small in

comparison with the wavelength. This would provide some justification for the continuum approach. Further, the computed velocity of fall for a glass sphere through the DC-200 is approximately 3×10^{-3} cm/sec; the observed velocity of the instability jets exceeds this Stokes particle velocity by a factor greater than 20. To further justify the continuum approach, we may also consider the effects of a single particle falling. In the previous case, the microorganism supports itself against gravity through the fluid, and it was demonstrated that all other actions by the cell were unimportant. In this example, the glass particle does not support itself, but independent motion by a particle can be ignored for two reasons. First, the independent motions would create disturbances only of the wavelength of nearest neighbor distance, already shown to be very short in comparison with the wavelengths of interest. Second, in a fluid with this high a concentration, one particle cannot move without effecting the motion of a number of other particles. Using an approximation to compute the first order interaction effects^[16] one finds for the ratio of interaction force to that of gravitational force for this concentration $F_I/F_g = 1.36$. Because the interaction force is great, no particle may move independently, and the fluid will act as a continuum.

VI. FURTHER COMMENTS ON BIOCONVECTION

A. INTRODUCTION

In the previous chapter, a model was presented for the pattern formation in cultures of microorganisms exhibiting negative geotaxis. No consideration was given to a steady state case where the cells swim back to the surface and a circulation exists. The preceding section was a model of a transient phenomenon; here a model of a steady state phenomenon is presented, and the use of the transient model is justified.

Experiments have been performed with biological cultures less than 1 cm in depth. In these cases, an instability is observed if the average concentration of cells is quite high ($> 10^5$ cells/cm³). In this situation, a clearly defined upper layer of increased concentration is not always observed; instead, a rather gentle, continuous concentration gradient occurs. In deeper cultures, mild concentration gradients also occur beneath the initial jump in concentration at the upper layer. A transient model of this situation is presented in this chapter, with an exponential density gradient taken as the continuous density variation. Only a simple model is presented, using a method similar to that employed in Chapter IV.

B. STEADY STATE CIRCULATION

A model for the steady state circulation patterns in Tetrahymena pyriformis may be adopted using several basic assumptions coupled with the careful use of experimental data. An important measurement for this application is that of the speed of the falling jets

of higher density fluid. In a typical case, this speed is about 0.1 cm/sec. If we assume that the concentration of protozoans in the upper layer remains constant, a model may be developed and some simple calculations performed to demonstrate that this assumption is both reasonable and produces good correlation with all the experimental results. This assumption implies that the number of cells lost through jets falling from the upper layer in unit time is equal to the number of cells that swim into the upper layer in unit time.

Several different phenomena come into play to create a steady state circulation. First, the jets begin to form in the upper layer. This is accompanied with the formation of polygon shaped patterns on the surface (see Fig. 12), with lines of greater concentration of cells forming the borders of the polygons. These lines carry the cells to the jets, which occur at the intersections of the lines. This behavior may be explained by the onset of the instability, which has been discussed previously. The formation of the polygon shapes, and a discussion of the patterns that may be formed is presented later in this chapter.

The second event is the growth of the jets into long, narrow fingers (see Fig. 11). We recall that the linearized theory predicts only a sinoidal wave with growing amplitude. The distortion of the wave into these fingers is due to nonlinear effects. This problem has not been solved for the viscous flow, but an approximation of the nonlinear effects with surface tension alone has been made [11]. Under this approximation, the preferred wavelength was unchanged, but the rate of growth and shape of the interface were modified.

The final phenomenon is the disintegration of the jets and return of the cells to the surface. Several effects can contribute to this return effect. The first possibility is that the jet may reach the bottom of the container and be stopped. When this occurs, the cells are no longer entrained and are free to swim back to the surface. Another possibility is that portions of the jet may be sheared away through viscous effects and the cells contained in this volume released. One other possible effect is that the cells simply swim out of the jets. The jet is quite narrow, being approximately 0.15 cm in width, and observations indicate that the jets shed cells as they descend. As the jets lose cells, the velocity of the jet decreases because the weight of the cells provides the driving force. Through any of these processes the results are the same: the cells are now in the lower fluid swimming towards the surface.

This process is a continuous cycle rather than a batch process. Cells enter the upper layer continuously, and are fed into jets and carried back into the lower fluid.

Some simple calculations demonstrate the success of this description. First, one may calculate the size of the jets in a typical case because the velocity of the jet is known. If we consider the drag on the jet, using a prolate spheroid model for the shape as a rough and simple approximation, we may calculate the diameter. The drag on a long, thin prolate spheroid of semimajor axis a and semiminor axis b falling end first with speed u is^[17]

$$f_d = \frac{4\pi\mu a}{\ln(a/b) + 0.193} . \quad (6.1)$$

We may use this force to match the gravitational force on the jet. The gravitational force is

$$f_g = 2\Delta \rho g \pi a b^2, \quad (6.2)$$

which takes bouyancy forces into account. At terminal velocity, these forces balance. The term $\ln(a/b)$ in the drag varies only slightly with changes in the ratio of length to width. For example, if $a/b = 10$, $\ln(a/b) = 2.3$. If $a/b = 50$, then $\ln a/b = 3.9$. An estimate that would seem to be reasonable is to take $\ln(a/b) + 0.193 \approx 3$. Thus we find

$$\frac{4\pi\mu u a}{3} = 2\Delta \rho g \pi a b^2, \quad (6.3)$$

or

$$b^2 = \frac{2\mu u}{3\Delta \rho g} . \quad (6.4)$$

From this result we see that the terminal velocity depends only on the width, not on the length. For our typical case, we have $\mu = 0.01$, $u = 0.1$, $\Delta \rho = 10^{-4}$, and $g = 10^3$, all in cgs units. These give the result that

$$b = 0.08 \text{ cm}, \quad (6.5)$$

where, as previously stated, b is the radius of the falling jet.

It must also be shown that the jet reaches this velocity in a short enough distance so that we may consider cells carried out of the upper layer to have this velocity. If the jet accelerates to this velocity with constant acceleration, we find

$$u(t) = \frac{\Delta \rho}{\rho_1 + \rho_2} gt = 0.05t. \quad (6.6)$$

To reach a speed of 0.1 cm/sec thus takes 2 secs. The distance traveled in this time is

$$d = \frac{1}{2} \frac{\Delta \rho}{\rho_1 + \rho_2} gt^2 = 0.1 \text{ cm}. \quad (6.7)$$

Thus, the velocity is reached in a very short distance, still within the upper layer.

We must now consider whether the continuous circulation model can produce results in good correlation with the observed results. The example we refer to has an upper layer concentration $C_u = 1.4 \times 10^6$ cells/cm³ and in the region just beneath the upper layer the concentration averages $C_m = 5.6 \times 10^5$ cells/cm³. The mean concentration of the culture is $C_o = 2.7 \times 10^5$ cells/cm³.

Through an area A of interface between the upper and lower layers, the flux out of the upper layer is

$$F_u^o = C_u u \Delta A, \quad (6.8)$$

where u is the speed of the falling jets, and ΔA is the area taken by the falling jets out of the total area A . If we recall that 17% of the

cells reaching the upper layer from below enter the upper layer, the flux from this middle layer to the upper is

$$F_u^i = 0.17 C_m u_o (A - \Delta A), \quad (6.9)$$

where $u_o = \alpha U$ is the projection of the swim speed, U , on the vertical, and $A - \Delta A$ is the area available for this inflow. For this case, the area of a single falling jet is $\pi b^2 = 0.02 \text{ cm}^2$. If in an area A the average distance between falling jets is λ , then A/λ^2 jets are present in A . Thus we find

$$\Delta A = \frac{\pi b^2 A}{\lambda^2}. \quad (6.10)$$

For this case $\lambda = 1 \text{ cm}$ (this is the average λ , not the minimum). The ratio of flux into the upper layer to that out of the upper layer is

$$\frac{F_u^i}{F_u^o} = \frac{0.17 C_m \alpha U (A - \Delta A)}{C_u u \Delta A}. \quad (6.11)$$

Substitution of the appropriate values gives $A/\Delta A = 50$, $U = 0.045 \text{ cm/sec}$, and

$$\frac{F_u^i}{F_u^o} = 1.5 \alpha. \quad (6.12)$$

If we require the flux ratio to be unity we find

$$\alpha = \frac{2}{3}. \quad (6.13)$$

If the upper layer has thickness h , the region with density C_m thickness h' , and the total depth of the fluid d , we may compute the concentration of cells in the lowest layer. The total number of cells is

$$N = C_o A d, \quad (6.14)$$

where C_o is the average concentration, A the area of the surface, and d the total depth. If we denote the concentration in the lowest layer as C_l , then

$$\frac{N}{A} = h C_u + h' C_m + (d - h - h') C_l = C_o d. \quad (6.15)$$

For this example $h = 0.1$ cm, $h' = 0.5$ cm, and $d = 2.0$ cm.

Equation (6.15) gives $C_l = 8.6 \times 10^4$ cells/cm³. It should be noted

that a density step does not exist between the middle and lower layer.

A mild, continuous gradient is present. The effects of such a gradient are calculated later in this chapter.

Computation of the flux into and out of the middle layer gives

$$F_m^o = 0.17 aU C_m, \quad (6.16)$$

and

$$F_m^i = aU C_l. \quad (6.17)$$

This ratio is

$$\frac{F_m^i}{F_m^o} = \frac{C_l}{0.17 C_m} = 0.935, \quad (6.18)$$

which is quite close to unity. The flux into and out of the lower layer is

$$\frac{F_{\ell}^i}{F_{\ell}^o} = \frac{C_u u \Delta A}{C_{\ell} \alpha U (A - \Delta A)} \quad (6.19)$$

For $\alpha = 2/3$, this is

$$\frac{F_{\ell}^i}{F_{\ell}^o} = 1.10, \quad (6.20)$$

which again is quite close to unity in view of the accuracy of other approximations. From the accuracy of the flux balance, one can see that this is a very plausible model for the steady state circulation.

To justify the use of a transient solution as a description of the circulation, we must examine the effects which are present in the steady state circulation but are ignored in the transient model. The first such effect is mass and momentum transfer due to the motion of the cells. As derived in Chapter V, these effects are several orders of magnitude below the static gravitational force, and may be neglected. The other effect we must consider is the mass transport of the medium. If we examine the calculations in this chapter, we find that the ratio of the area of falling jets to the area available for return flow is 1:50. From continuity considerations, this means that the velocity of the fluid medium (excluding the jets) is quite small; and in the present case it is 0.002 cm/sec. This velocity is small enough to be ignored, for if we take a time scale of one or two minutes, the bulk of the fluid has not moved significantly, yet the cells have gone

through several cycles. If one wishes to attempt a solution for time periods much longer than some minutes, this flow may play a role, and other effects would also have to be considered. One such effect is reproduction and death of cells. If one wished to model the flow over the period of an hour or so, the population of the culture could change significantly during that time. In highly concentrated cultures, toxins accumulate which can cause a large proportion of cells to die; in a fresh medium, the population doubles in three hours for Tetrahymena pyriformis. Thus we assume that the model used here is valid for time scales of a few minutes, or for several round trips by an individual cell.

This slow return flow calculation points out an important difference between this circulation and other convection problems. In the present case, the flow of the medium is very small, and we are concerned primarily with the circulation of cells. Thermal convection, which is the driving mechanism for Bénard cells, is a circulation of the entire medium. For the microorganism example, the cells swim upward with a speed over twenty times that of the return liquid flow.

A calculation may be made of the minimum value which the density difference may have for the instability to occur. The theoretical results indicate that any situation is unstable when a heavy fluid is above a lighter fluid in the absence of surface tension. This theory does not take the swimming of the microorganisms into account. If a very slight density difference is present, jets could form and fall, but the rate of fall would be quite slow. If this were the case, the

cells could swim back up faster than they are being carried down. This limiting density difference is computed to be of the same magnitude as the observed cutoff density difference.

The irregular polygon shapes on the surface (see Fig. 12) may be accounted for easily. This phenomenon is not due to either steady state effects or nonlinear effects. The linearized theory predicts a preferred wavelength, but it is a two dimensional model. What the theory actually predicts is the distance between parallel wave crests on the interface. Because no direction is preferred, lines of waves propagate in arbitrary directions, and these lines intersect forming the polygons. In the two dimensional theory the greatest growth occurs on these wave crests; in the three dimensional experiment it occurs at the intersection points of the crests. The patterns are in addition affected by the container boundary. In most of the experiments which we have seen the container size is less than an order of magnitude larger than the theoretical wavelength.

C. EXPONENTIAL DENSITY GRADIENTS

Bioconvection experiments in cultures less than 1.0 cm in depth do not show evidence of a clearly defined upper layer with higher than average concentration. These experiments indicate that an unstable density gradient exists throughout the depth of the fluid. As was previously noted earlier in this chapter, mild concentration gradients also occur in deeper cultures below the initial density step at the interface. By use of simple techniques similar to those in Chapter IV, these cases may be modeled for an assumed exponential density gradient.

The inviscid solution for a fluid of finite thickness with an exponential density gradient was first given by Rayleigh^[4]. This solution is as follows.

If we take the same coordinate system used previously, with a horizontal x axis and a vertical y axis, such that $y = 0$ is the lower boundary of the fluid, and $y = d$ the upper surface, and take the pressure to be of the form $P + \delta P$, where P is a function of depth alone, and the density $\rho + \delta\rho$ with ρ a function of depth only, we find that

$$-\frac{1}{\rho} \frac{\partial P}{\partial y} - g = 0, \quad (6.21)$$

for the rest condition. The equation of continuity is

$$\frac{\partial}{\partial t} (\rho + \delta\rho) + (\rho + \delta\rho) \frac{\partial u_i}{\partial x_i} + v \frac{\partial}{\partial y} (\rho + \delta\rho) = 0. \quad (6.22)$$

If we keep only terms of first order, and make the Boussinesq approximation, we find

$$\frac{\partial u_i}{\partial x_i} = 0, \quad (6.23)$$

and

$$\frac{\partial(\rho + \delta\rho)}{\partial t} = \frac{\partial\delta\rho}{\partial t} = -v \frac{\partial\rho}{\partial y}. \quad (6.24)$$

The linearized equations of motion are

$$\rho \frac{\partial u_i}{\partial t} = - \frac{\partial\delta P}{\partial x_i} - g\delta\rho \hat{y}, \quad (6.25)$$

where \hat{y} is the unit vector in the upward vertical direction. If we let $D = \frac{d}{dy}$, then the equations become

$$\rho \frac{\partial u}{\partial t} = - \frac{\partial \delta P}{\partial x}, \quad (6.26)$$

$$\rho \frac{\partial v}{\partial t} = - \frac{\partial \delta P}{\partial y} - g \delta \rho, \quad (6.27)$$

$$\frac{\partial u}{\partial x} + \frac{\partial v}{\partial y} = 0, \quad (6.28)$$

and

$$\frac{\partial \delta \rho}{\partial t} = - v D \rho. \quad (6.29)$$

If we assume that the functions have a dependence on x and t of the form $\exp(i\kappa x + nt)$, these equations become

$$\rho n u = -i\kappa \delta P, \quad (6.30)$$

$$\rho n v = - \frac{\partial}{\partial y} \delta P - g \delta \rho, \quad (6.31)$$

$$i\kappa u = - D v, \quad (6.32)$$

and

$$n \delta \rho = - v D \rho. \quad (6.33)$$

If we multiply (6.30) by $i\kappa$, and use (6.32), the result is

$$- \rho n D v = \kappa^2 \delta P. \quad (6.34)$$

Elimination of $\delta \rho$ between (6.31) and (6.33) gives

$$\rho n v = - \frac{\partial}{\partial y} \delta P + \frac{v g}{n} D \rho. \quad (6.35)$$

Combining (6.34) and (6.35) to remove δP gives

$$D(\rho Dv) = \rho \kappa^2 v - \frac{vg\kappa^2 D\rho}{n^2}. \quad (6.36)$$

If we substitute $\rho = \rho_0 e^{\beta y}$ into this equation, we find

$$D^2 v + \beta Dv - \kappa^2 (1 - g\beta/n^2) v = 0. \quad (6.37)$$

A solution may be found of the form

$$v = e^{i\kappa x + nt} [Ae^{q_1 y} + Be^{q_2 y}], \quad (6.38)$$

where

$$q_1 = \frac{1}{2} \{-\beta + [\beta^2 + 4\kappa^2(1 - g\beta/n^2)]^{\frac{1}{2}}\}, \quad (6.39)$$

and

$$q_2 = \frac{1}{2} \{-\beta - [\beta^2 + 4\kappa^2(1 - g\beta/n^2)]^{\frac{1}{2}}\}. \quad (6.40)$$

The appropriate condition at the lower surface is $v = 0$ at $y = 0$.

This gives

$$v = Ae^{i\kappa x + nt} [e^{q_1 y} - e^{q_2 y}]. \quad (6.41)$$

The appropriate condition at the upper surface is $v = 0$ at $y = d$ for the rigid boundary case, and $\frac{\partial}{\partial t} (P + \delta P) = 0$ at $y = d$ for the free surface case. This second case is equivalent to

$$n^2 Dv + g\kappa^2 v = 0 \quad \text{at } y = d. \quad (6.42)$$

In our example, we may neglect the first term in (6.42) because, for $\beta \approx 10^{-4}$, we have

$$\frac{n^2 Dv}{g\kappa} + v \approx \left(\frac{n^2 q}{g\kappa} + 1 \right) v = 0 \Big|_{y=d}. \quad (6.43)$$

In the region of interest,

$$\left| \frac{n^2 q}{g\kappa} \right| < 10^{-4}, \quad (6.44)$$

where the absolute value has been taken because q_1 and q_2 are complex. With this simplification, the free surface condition is the same as that for the rigid boundary: $v = 0$ at $y = d$. This condition yields

$$v \Big|_{y=d} = A e^{ikx + nt} \left[e^{q_1 d} - e^{q_2 d} \right] = 0, \quad (6.45)$$

which is equivalent to

$$\exp [(q_1 - q_2)d] = 1, \quad (6.46)$$

or

$$(q_1 - q_2)d = 2im\pi, \quad (6.47)$$

where m is any integer. Simplification of this result leads to the following:

$$v = A' e^{-\frac{1}{2}\beta y} \sin \left(\frac{m\pi y}{d} \right), \quad (6.48)$$

where A' is a constant. Thus, for $m = 0$ no motion is present.

Equations (6.39), (6.40), and (6.47) give

$$n^2 = \frac{g\beta\kappa^2 d^2}{\kappa^2 d^2 + \frac{1}{4}\beta^2 d^2 + m^2 \pi^2}, \quad (6.49)$$

where $m = 1, 2, 3$, etc. If $\beta > 0$, the fluid is unstable and n is real. If $\beta < 0$, n is purely imaginary, and oscillations occur which are familiar as Brunt-Väisälä modes. For the unstable case, we are only interested in the fastest growing instability which occurs for $m = 1$.

A method similar to that employed in Chapter IV may be used here; we may write

$$n^2 + 2\nu\kappa^2 n - \frac{g\beta\kappa^2 d^2}{\kappa^2 d^2 + \frac{1}{4}\beta^2 d^2 + \pi^2} = 0. \quad (6.50)$$

If we let $\kappa' = \kappa d$, $\beta' = \beta d$, $n' = n/(\beta g)^{\frac{1}{2}}$, and $\nu' = \nu/d^2(\beta g)^{\frac{1}{2}}$, then a nondimensional form of (6.50) is

$$n'^2 + 2\nu'\kappa'^2 n' - \frac{\kappa'^2}{\kappa'^2 + \frac{1}{4}\beta'^2 + \pi^2} = 0. \quad (6.51)$$

Figure 14 shows n' versus κ' for the case where $d = 1$ cm, $\beta = 5.9 \times 10^{-4}/\text{cm}$, $g = 10^3 \text{ cm/sec}^2$, and $\nu = 0.01 \text{ cm}^2/\text{sec}$. From this graph we see that n' is a maximum for $\kappa' \approx 4$, which corresponds to $\lambda \approx 1.6$ cm, a result similar to those obtained in the density step calculations.

This calculation indicates that for cultures in shallow dishes, the wavelength may again be predicted, however, no accurate

experiments have been performed with these shallow cultures, so correlation of this result with experimental evidence is not possible. If appropriate numbers are substituted to describe the middle layer of the fluid described previously, one finds a preferred wavelength, but the growth rate at which this disturbance increases is not as great as the corresponding growth rate at the density step interface. For this reason, one would expect to observe the instability at the interface.

One aspect of the stable case was commented on by Rayleigh, and is quite unusual. If one examines the character of the solution for the stable case in the absence of viscosity, it is observed that an upper limit exists on the frequency of vibrations, but that no lower limit exists, the opposite of most physical systems.

VII. SUMMARY AND CONCLUSIONS

It has been shown that Rayleigh-Taylor instability can lead to pattern formation similar to Bénard cells, but that the patterns are quite dependent on viscosity. The theory that has been developed has been shown to produce excellent correlation with experimental results. The approximate solutions have also been shown to be quite good, and are far more convenient to use than the exact solution. These approximations are summarized at the end of Chapter III.

Bioconvection in microorganism cultures has been modeled with excellent correlation with observations. The special cases of steady state microorganism circulation and the culture with an exponential density gradient have also been discussed, with calculations performed to demonstrate how these situations effect the model of circulation previously developed. While the biological case was modeled successfully, a number of other physical processes not discussed may also be described under the general techniques derived within this paper. Several of these are circulation in an unstable atmosphere or ocean. Although some modification may be needed to describe these cases, the approximations could prove quite useful for qualitative descriptions of the motion.

APPENDIX A

REDUCTION OF THE FOUR BY FOUR DETERMINANT - EQUATION

(2.48)

The determinant is

$$\begin{vmatrix}
 1 & 1 & 1 & -1 \\
 \kappa & m_1 & -\kappa & m_2 \\
 2\mu_1\kappa^2 & \mu_1(m_1^2 + \kappa^2) & 2\mu_2\kappa^2 & -\mu_2(m_2^2 + \kappa^2) \\
 \beta/n - \rho_1 n - 2\mu_1\kappa^2 & \beta/n - 2\mu_1\kappa m_1 & \rho_2 n + 2\mu_2\kappa^2 & -2\mu_2\kappa m_2
 \end{vmatrix} = 0,$$

(A. 1)

where $\beta = g\Delta\rho\kappa - T\kappa^3$.

If one subtracts the first column from the second, adds the third column to the fourth, then subtracts the first column from the third, the result is

$$\begin{vmatrix}
 1 & 0 & 0 & 0 \\
 \kappa & m_1 - \kappa & -2\kappa & m_2 - \kappa \\
 2\mu_1\kappa^2 & \mu_1(m_1^2 - \kappa^2) & 2\kappa^2(\mu_2 - \mu_1) & \mu_2(\kappa^2 - m_2^2) \\
 \beta/n - \rho_1 n - 2\mu_1\kappa^2 & -2\mu_1\kappa m_1 + \rho_1 n + 2\mu_1\kappa^2 & (\rho_1 + \rho_2)n + 2\kappa^2(\mu_1 + \mu_2) - \beta/n & \rho_2 n + 2\mu_2\kappa(\kappa - m_2)
 \end{vmatrix} = 0.$$

(A. 2)

This is equivalent to the three by three determinant obtained by omitting the first row and column. Some simplification results if one notes that

$$\mu_1(m_1^2 - \kappa^2) = \mu_1(\kappa^2 + \frac{n\rho_1}{\mu_1} - \kappa^2) = n\rho_1 \quad (\text{A. 3})$$

and

$$\mu_2(\kappa^2 - m_2^2) = \mu_2(\kappa^2 - \kappa^2 - n\rho_2/\mu_2) = -n\rho_2. \quad (\text{A. 4})$$

The resulting three by three determinant is

$$\begin{vmatrix} m_1 - \kappa & -2\kappa & m_2 - \kappa \\ \rho_1^n & -2\Delta\mu\kappa^2 & -\rho_2^n \\ \rho_1^{n+2\mu_1\kappa(\kappa-m_1)} & n(\rho_1 + \rho_2) + 2(\mu_1 + \mu_2)\kappa^2 - \beta/n & \rho_2^{n+2\mu_2\kappa(\kappa-m_2)} \end{vmatrix} = 0, \quad (\text{A. 5})$$

where $\Delta\mu = \mu_1 - \mu_2$ as before.

Subtracting the first and third columns from the second gives

$$\begin{vmatrix} m_1 - \kappa & -(m_1 + m_2) & m_2 - \kappa \\ \rho_1^n & -2\Delta\mu\kappa^2 - n\Delta\rho & -\rho_2^n \\ \rho_1^{n+2\mu_1\kappa(\kappa-m_1)} & -\beta/n + 2\mu_1\kappa m_1 + 2\mu_2\kappa m_2 & \rho_2^{n+2\mu_2\kappa(\kappa-m_2)} \end{vmatrix} = 0, \quad (\text{A. 6})$$

where $\Delta\rho = \rho_1 - \rho_2$ as before.

Multiplication of the second column by $-n/\kappa$, and division of the second row by n gives Eq. (2.49):

$$\begin{vmatrix} m_1 - \kappa & \frac{n}{\kappa} (m_1 + m_2) & m_2 - \kappa \\ \rho_1 & 2\kappa\Delta\mu + \frac{n\Delta\rho}{\kappa} & -\rho_2 \\ \rho_1^{n+2\mu_1\kappa(\kappa-m_1)} & \beta/\kappa - 2n(\mu_1 m_1 + \mu_2 m_2) & \rho_2^{n+2\mu_2\kappa(\kappa-m_2)} \end{vmatrix} = 0. \quad (\text{A. 7})$$

Expanding by minors, one finds

$$\begin{aligned} & (m_1 - \kappa) \left[(2\kappa\Delta\mu + \frac{n\Delta\rho}{\kappa})(\rho_2^n + 2\mu_2\kappa(\kappa - m_2)) + \rho_2(\beta/\kappa - 2n(\mu_1 m_1 + \mu_2 m_2)) \right] \\ & + \frac{n}{\kappa}(m_1 + m_2) \left[-\rho_2(\rho_1^n + 2\mu_1\kappa(\kappa - m_1)) - \rho_1(\rho_2^n + 2\mu_2\kappa(\kappa - m_2)) \right] \\ & + (m_2 - \kappa) \left[\rho_1(\beta/\kappa - 2n(\mu_1 m_1 + \mu_2 m_2)) - (2\kappa\Delta\mu + \frac{n\Delta\rho}{\kappa})(\rho_1^n + 2\mu_1\kappa(\kappa - m_1)) \right] \\ & = 0. \quad (\text{A. 8}) \end{aligned}$$

Expanding inside the square brackets gives

$$\begin{aligned} & (m_1 - \kappa) \left[2\kappa\Delta\mu\rho_2^n + 4\mu_2\Delta\mu\kappa^3 - 4\mu_2\Delta\mu\kappa^2 m_2 + \frac{\Delta\rho\rho_2}{\kappa} n^2 + 2\mu_2\kappa\Delta\rho n - 2\mu_2 m_2 \Delta\rho n \right. \\ & \quad \left. + \rho_2\beta/\kappa - 2\rho_2\mu_1 m_1 n - 2\rho_2\mu_2 m_2 n \right] \\ & + \frac{n}{\kappa}(m_1 + m_2) \left[-\rho_1\rho_2^{n-2\mu_1\kappa} \rho_2^2 + 2\mu_1\kappa m_1 \rho_2 - \rho_1\rho_2^n - 2\mu_2\kappa^2 \rho_1^2 + 2\mu_2\kappa m_2 \rho_2 \right] \\ & + (m_2 - \kappa) \left[\rho_1\beta/\kappa - 2\rho_1\mu_1 m_1 n - 2\rho_1\mu_2 m_2 n - 2\kappa\Delta\mu\rho_1 n - 4\kappa^3 \Delta\mu\mu_1 + 4\kappa^2 \Delta\mu\mu_1 m_1 \right. \\ & \quad \left. - \Delta\rho\rho_1 n^2/\kappa - 2\mu_1\kappa\Delta\rho n + 2\mu_1\Delta\rho m_1 n \right] = 0. \quad (\text{A. 9}) \end{aligned}$$

If we temporarily ignore the fact that the m_1 and m_2 terms contain n , and collect terms as coefficients of either n^2 , n^1 , or n^0 , those terms that are coefficients of n^2

$$= [m_1 \Delta \rho \rho_2 / \kappa - \Delta \rho \rho_2 - 2m_1 \rho_1 \rho_2 / \kappa - 2m_2 \frac{\rho_1}{\kappa} \rho_2 - m_2 \frac{\Delta \rho \rho_1}{\kappa} + \Delta \rho \rho_1]. \quad (\text{A. 10})$$

Simplifying and reordering, this is,

$$= [(-\Delta \rho \rho_2 + \Delta \rho \rho_1) + 1/\kappa [m_1 (\rho_1 \rho_2 - \rho_2^2 - 2\rho_1 \rho_2) + m_2 (-2\rho_1 \rho_2 - \rho_1^2 + \rho_1 \rho_2)]]. \quad (\text{A. 11})$$

So this coefficient becomes

$$= [(\Delta \rho)^2 - \frac{1}{\kappa} (\rho_1 + \rho_2)(m_1 \rho_2 + m_2 \rho_1)]. \quad (\text{A. 12})$$

The coefficient of the n^1 term is

$$\begin{aligned} &= 2[\kappa \Delta \mu \rho_2 m_1 - \kappa^2 \Delta \mu \rho_2 + \mu_2 \kappa \Delta \rho m_1 - \mu_2 \kappa^2 \Delta \rho - \mu_2 m_2 m_1 \Delta \rho + \mu_2 m_2 \kappa \Delta \rho \\ &- \rho_2 \mu_1 m_1^2 + \rho_2 \mu_1 m_1 \kappa - \rho_2 \mu_2 m_1 m_2 + \rho_2 \mu_2 m_2 \kappa - \mu_1 \kappa m_1 \rho_2 - \mu_1 \rho_2 \kappa m_2 \\ &+ \mu_1 \rho_2 m_1^2 + \mu_1 \rho_2 m_1 m_2 - \mu_2 \rho_1 \kappa m_1 - \mu_2 \rho_1 \kappa m_2 + \mu_2 \rho_1 m_1 m_2 + \mu_2 \rho_1 m_2^2 \\ &- \rho_1 \mu_1 m_1 m_2 + \rho_1 \mu_1 m_1 \kappa - \rho_1 \mu_2 m_2^2 + \rho_1 \mu_2 m_2 \kappa - \Delta \mu \rho_1 \kappa m_2 + \Delta \mu \rho_1 \kappa^2 \\ &- \mu_1 \kappa \Delta \rho m_2 + \mu_1 \Delta \rho \kappa^2 + \mu_1 \Delta \rho m_1 m_2 - \mu_1 \Delta \rho m_1 \kappa]. \end{aligned} \quad (\text{A. 13})$$

Regrouping these terms by the coefficients m_1^2 , $m_1 m_2$, m_2^2 , $m_1 \kappa$, $m_2 \kappa$, and κ^2 this is

$$\begin{aligned}
 &= 2[m_1^2 (-\rho_2\mu_1 + \mu_1\rho_2) + m_2^2 (\mu_2\rho_1 - \rho_1\mu_2) + m_1m_2(-\mu_2\Delta\rho - \rho_2\mu_2 \\
 &+ \mu_1\rho_2 + \mu_2\rho_1 - \rho_1\mu_1 + \mu_1\Delta\rho) + m_1\kappa(\Delta\mu\rho_2 + \mu_2\Delta\rho + \rho_2\mu_1 - \mu_1\rho_2 - \mu_2\rho_1 \\
 &+ \rho_1\mu_1 - \mu_1\Delta\rho) + m_2\kappa(\mu_2\Delta\rho + \rho_2\mu_2 - \mu_1\rho_2 - \mu_2\rho_1 + \rho_1\mu_2 - \Delta\mu\rho_1 - \mu_1\Delta\rho) \\
 &+ \kappa^2(-\Delta\mu\rho_2 - \mu_2\Delta\rho + \Delta\mu\rho_1 + \mu_1\Delta\rho)]. \tag{A. 14}
 \end{aligned}$$

Upon reduction, this is

$$= 2(\Delta\mu\kappa)[\Delta\rho(2\kappa - m_1 - m_2) + (\rho_1 + \rho_2)(m_1 - m_2)]. \tag{A. 15}$$

The coefficient of n^0 is

$$\begin{aligned}
 &= [4\mu_2\Delta\mu\kappa^3m_1 - 4\mu_2\Delta\mu\kappa^4 - 4\mu_2\Delta\mu\kappa^2m_1m_2 + 4\mu_2\Delta\mu\kappa^3m_2 \\
 &+ \rho_2\beta m_1/\kappa - \rho_2\beta + \rho_1\frac{\beta m_2}{\kappa} - \rho_1\beta - 4\kappa^3\Delta\mu\mu_1m_2 + 4\kappa^4\Delta\mu\mu_1 \\
 &+ 4\kappa^2\Delta\mu\mu_1m_1m_2 - 4\kappa^3\Delta\mu\mu_1m_1], \tag{A. 16}
 \end{aligned}$$

$$\begin{aligned}
 &= \beta\left[\frac{1}{\kappa}(\rho_1m_2 + \rho_2m_1) - (\rho_1 + \rho_2)\right] + 4\kappa^2\Delta\mu[\mu_2\kappa m_1 - \mu_2\kappa^2 \\
 &- \mu_2m_1m_2 + \mu_2\kappa m_2 - \kappa\mu_1m_1 + \kappa^2\mu_1 + \mu_1m_1m_2 - \kappa\mu_1m_1], \tag{A. 17}
 \end{aligned}$$

$$= \beta/\kappa[(\rho_1m_2 + \rho_2m_1) - \kappa(\rho_1 + \rho_2)] + 4\kappa^2(\Delta\mu)^2(\kappa - m_1)(\kappa - m_2). \tag{A. 18}$$

So the resultant equation is

$$\begin{aligned} & n^2 \left[(\Delta \rho)^2 - \frac{(\rho_1 + \rho_2)}{\kappa} (m_1 \rho_2 + m_2 \rho_1) \right] \\ & + n [2\kappa \Delta \mu] [\Delta \rho (2\kappa - m_1 - m_2) + (\rho_1 + \rho_2)(m_1 - m_2)] \quad (\text{A. 19}) \\ & + \beta/\kappa [(\rho_1 m_2 + \rho_2 m_1) - (\rho_1 + \rho_2) \kappa] + 4\kappa^2 (\Delta \mu)^2 (\kappa - m_1)(\kappa - m_2) = 0. \end{aligned}$$

APPENDIX B

EXPANSION OF EQUATION (2.50)

Equation (2.50) is

$$\begin{aligned}
 & n^2 [(\Delta \rho)^2 - \frac{(\rho_1 + \rho_2)}{\kappa} (m_1 \rho_2 + m_2 \rho_1)] \\
 & + n [2\kappa \Delta \mu] [\Delta \rho (2\kappa - m_1 - m_2) + (\rho_1 + \rho_2)(m_1 - m_2)] \quad (B.1) \\
 & + \beta/\kappa [(\rho_1 m_2 + \rho_2 m_1) - (\rho_1 + \rho_2)\kappa] + 4\kappa^2 (\Delta \mu)^2 (\kappa - m_1)(\kappa - m_2) = 0.
 \end{aligned}$$

If we require

$$\frac{\mu_1}{\rho_1} = \frac{\mu_2}{\rho_2} = \nu, \quad (B.2)$$

then

$$m_1 = m_2 = (\kappa^2 + n/\nu)^{\frac{1}{2}} \quad (B.3)$$

and

$$\Delta \mu = \nu \Delta \rho. \quad (B.4)$$

The notation

$$\rho' = \rho_1 + \rho_2 \quad (B.5)$$

will be used. Grouping those terms that are coefficients of m , Eq.

(B.1) becomes

$$\begin{aligned}
 & m \left[\frac{\rho'^2 n^2}{\kappa} + 4n\kappa \nu (\Delta \rho)^2 - \rho' \beta/\kappa + 8\kappa^3 \nu^2 (\Delta \rho)^2 \right] \\
 & = [(\Delta \rho)^2 n^2 + 4\kappa^2 \nu (\Delta \rho)^2 n - \beta \rho' + 4\kappa^2 \nu^2 (\Delta \rho)^2 (\kappa^2 + m^2)], \quad (B.6)
 \end{aligned}$$

$$= [(\Delta \rho)^2 n^2 + 8\kappa^2 \nu (\Delta \rho)^2 n - \beta \rho' + 8\kappa^4 \nu^2 (\Delta \rho)^2]. \quad (\text{B. 7})$$

Squaring both sides of (B. 7) gives

$$\begin{aligned} & (\kappa^2 + \frac{n}{\nu}) \left[\frac{\rho'^4 n^4}{\kappa^2} + 16n^2 \kappa^2 \nu^2 (\Delta \rho)^4 + \frac{\beta^2 \rho'^2}{\kappa^2} + 64\kappa^6 \nu^4 (\Delta \rho)^4 \right. \\ & + 8n^3 \rho'^2 (\Delta \rho)^2 \nu - \frac{2n^2 \beta \rho'^3}{\kappa} + 16n^2 \rho'^2 (\Delta \rho)^2 \kappa^2 \nu^2 - 8n\nu (\Delta \rho)^2 \rho' \beta \\ & \left. + 64n\kappa^4 \nu^3 (\Delta \rho)^4 - 16\beta \rho' \kappa^2 \nu^2 (\Delta \rho)^2 \right] \quad (\text{B. 8}) \end{aligned}$$

$$\begin{aligned} & = [(\Delta \rho)^4 n^4 + 64\kappa^4 \nu^2 (\Delta \rho)^4 n^2 + \beta^2 \rho'^2 + 64\kappa^8 \nu^4 (\Delta \rho)^4 \\ & + 16(\Delta \rho)^4 \nu \kappa^2 n^3 - 2\beta \rho' (\Delta \rho)^2 + 16\kappa^4 \nu^2 (\Delta \rho)^4 n^2 - 16\kappa^2 \nu (\Delta \rho)^2 \rho' \beta n \\ & + 128\kappa^6 \nu^3 (\Delta \rho)^4 n - 16\beta \rho' \kappa^4 \nu^2 (\Delta \rho)^2]. \end{aligned}$$

Regrouping by like powers of n , one finds

$$\begin{aligned} & n^5 \left[\rho'^4 / \nu \kappa^2 \right] + n^4 \left[\rho'^4 + 8\rho'^2 (\Delta \rho)^2 - (\Delta \rho)^4 \right] + n^3 \left[16\kappa^2 \nu (\Delta \rho)^4 + 8\rho'^2 (\Delta \rho)^2 \nu \kappa^2 \right. \\ & - \frac{2\beta \rho'^3}{\nu \kappa} + 16\rho'^2 (\Delta \rho)^2 \nu \kappa^2 - 16(\Delta \rho)^4 \nu \kappa^2 \left. \right] + n^2 \left[16\kappa^4 \nu^2 (\Delta \rho)^4 - 2\beta \rho'^3 \right. \\ & + 16\rho'^2 (\Delta \rho)^2 \nu^2 \kappa^4 - 8\beta \rho' (\Delta \rho)^2 + 64\kappa^4 \nu^2 (\Delta \rho)^4 - 64\kappa^4 \nu^2 (\Delta \rho)^4 + 2\beta \rho' (\Delta \rho)^2 \\ & - 16\nu^2 \kappa^4 (\Delta \rho)^4 \left. \right] + n \left[\beta^2 \rho'^2 / \nu \kappa^2 + 64\nu^3 \kappa^6 (\Delta \rho)^4 - 8\nu \kappa^2 (\Delta \rho)^2 \rho' \beta \right. \\ & + 64\nu^3 \kappa^6 (\Delta \rho)^4 - 16\beta \rho' \nu \kappa^2 (\Delta \rho)^2 + 16\nu \kappa^2 (\Delta \rho)^2 \rho' \beta - 128\nu^3 \kappa^2 (\Delta \rho)^4 \left. \right] \\ & + \left[\beta^2 \rho'^2 + 64\kappa^8 \nu^4 (\Delta \rho)^4 - 16\beta \rho' \kappa^4 \nu^2 (\Delta \rho)^2 - \beta^2 \rho'^2 - 64\kappa^8 \nu^4 (\Delta \rho)^4 \right. \\ & \left. + 16\beta \rho' \kappa^4 \nu^2 (\Delta \rho)^2 \right] = 0. \quad (\text{B. 9}) \end{aligned}$$

Under simplification, this becomes

$$\begin{aligned}
 & n^5 [\rho'^4/\nu\kappa^2] + n^4 [\rho'^4 - (\Delta\rho)^4 + 8\rho'^2(\Delta\rho)^2] + n^3 [24\rho'^2(\Delta\rho)^2 \nu\kappa^2 \\
 & - 2\beta\rho'^3/\nu\kappa^2] + n^2 [-2\beta\rho'^3 - 6\beta\rho'(\Delta\rho)^2 + 16\rho'^2(\Delta\rho)^2 \nu^2\kappa^4] + n [\beta^2\rho'^2/\nu\kappa^2 \\
 & - 8\nu\kappa^2(\Delta\rho)^2\rho'\beta] + [0] = 0. \tag{B.10}
 \end{aligned}$$

If one divides (B.10) by $\rho'^4 \nu^3 \kappa^6 n$, the result is

$$\begin{aligned}
 & \left(\frac{n}{\nu\kappa}\right)^4 + \left(\frac{n}{\nu\kappa}\right)^3 \left[1 - \left(\frac{\Delta\rho}{\rho'}\right)^4 + 8\left(\frac{\Delta\rho}{\rho'}\right)^2\right] + \left(\frac{n}{\nu\kappa}\right)^2 \left[24\left(\frac{\Delta\rho}{\rho'}\right)^2 - \frac{2\beta}{\rho'\nu^2\kappa^4}\right] \\
 & + \left(\frac{n}{\nu\kappa}\right) \left[\frac{-2\beta}{\rho'\nu^2\kappa^4} - \frac{6\beta}{\rho'\nu^2\kappa^4} \left(\frac{\Delta\rho}{\rho'}\right)^2 + 16\left(\frac{\Delta\rho}{\rho'}\right)^2\right] + \left[\frac{\beta^2}{\rho'\nu^4\kappa^8} - \frac{8\beta}{\rho'\nu^2\kappa^4} \left(\frac{\Delta\rho}{\rho'}\right)^2\right] = 0. \tag{B.11}
 \end{aligned}$$

We define the following dimensionless quantities:

$$z = n/\nu\kappa^2, \tag{B.12}$$

$$a = \beta/\rho'\nu^2\kappa^4, \tag{B.13}$$

and

$$\gamma = \Delta\rho/\rho', \tag{B.14}$$

to give the final result,

$$\begin{aligned}
 & z^4 + z^3 [1 - \gamma^4 + 8\gamma^2] + z^2 [24\gamma^2 - 2a] \\
 & + z [-2a - 6\gamma^2 a + 16\gamma^2] + [a^2 - 8\gamma^2 a] = 0. \tag{B.15}
 \end{aligned}$$

APPENDIX C

DERIVATION OF $\omega_o = (g\kappa)^{\frac{1}{2}}$

The equations describing the fluid are

$$\frac{\partial u}{\partial x} + \frac{\partial v}{\partial y} = 0, \quad (C. 1)$$

$$\frac{\partial u}{\partial t} = -\frac{1}{\rho} \frac{\partial P}{\partial x}, \quad (C. 2)$$

and

$$\frac{\partial v}{\partial t} = -\frac{1}{\rho} \frac{\partial P}{\partial y} - g, \quad (C. 3)$$

where $g > 0$.

If

$$u = -\frac{\partial \varphi}{\partial x} \quad (C. 4)$$

and

$$v = -\frac{\partial \varphi}{\partial y} \quad (C. 5)$$

then by Eq. (C. 1),

$$\nabla^2 \varphi = 0. \quad (C. 6)$$

The substitution of Eq. (C. 5) into (C. 3), and integration of the result gives

$$P = P_o + \rho \frac{\partial \varphi}{\partial t} - \rho g y. \quad (C. 7)$$

The surface disturbance η , is taken to be

$$\eta = a e^{i\omega t} \cos \kappa x. \quad (C. 8)$$

The velocity must die out as $y \rightarrow -\infty$, so we choose

$$\varphi = Ae^{\kappa y} e^{i\omega t} \cos \kappa x. \quad (\text{C. 9})$$

Two conditions which apply are

$$P = P_0 \Big|_{y=\eta} \quad (\text{C. 10})$$

and

$$\frac{\partial \eta}{\partial t} = - \frac{\partial \varphi}{\partial y} \Big|_{y=0} \quad (\text{C. 11})$$

From Eq. (C. 11) one finds

$$i\omega a = -\kappa A. \quad (\text{C. 12})$$

Equations (C. 12), (C. 7), and (C. 10) give

$$\rho i\omega A - g\rho a = 0, \quad (\text{C. 13})$$

which gives

$$-(i\omega)^2 \rho \frac{a}{\kappa} - g\rho a = 0, \quad (\text{C. 14})$$

and this result yields

$$\omega^2 = g\kappa. \quad (\text{C. 15})$$

APPENDIX D

DERIVATION THAT $\omega_o = \{g\kappa(\rho_2 - \rho_1)/(\rho_2 + \rho_1)\}^{\frac{1}{2}}$

Proceeding in a manner similar to that of Appendix C gives

$$\varphi_1 = A_1 e^{-\kappa y} e^{i\omega t} \cos \kappa x, \quad (D. 1)$$

$$\varphi_2 = A_2 e^{+\kappa y} e^{i\omega t} \cos \kappa x, \quad (D. 2)$$

and

$$\eta = a e^{i\omega t} \cos \kappa x, \quad (D. 3)$$

with

$$i\omega a = \kappa A_1 = -\kappa A_2. \quad (D. 4)$$

The pressure is

$$P_1 = P_o + \rho_1 \frac{\partial \varphi_1}{\partial t} - \rho_1 g y \quad (D. 5)$$

$$P_2 = P_o + \rho_2 \frac{\partial \varphi_2}{\partial t} - \rho_2 g y. \quad (D. 6)$$

At the interface, $P_1 = P_2$, which gives

$$\rho_1 i\omega A_1 - \rho_1 g a = \rho_2 i\omega A_2 - \rho_2 g a. \quad (D. 7)$$

This gives the expected result

$$\omega^2 = g\kappa \frac{\rho_2 - \rho_1}{\rho_2 + \rho_1}. \quad (D. 8)$$

When surface tension is acting the condition at the interface becomes

$$P_1 - T \frac{\partial^2 \eta}{\partial x^2} = P_2, \quad (\text{D. 9})$$

and as a result,

$$i\omega A_1 \rho_1 - \rho_1 g a + T \kappa^2 a = i\omega A_2 \rho_2 - \rho_2 g a. \quad (\text{D. 10})$$

Equation (D. 4) simplifies (D. 10) to the form

$$-\frac{\omega^2}{\kappa} \rho_1 - \rho_1 g + T \kappa^2 = \frac{\omega^2}{\kappa} \rho_2 - \rho_2 g,$$

or

$$\omega^2 = g\kappa \frac{(\rho_2 - \rho_1)}{(\rho_2 + \rho_1)} + \frac{T\kappa^3}{(\rho_2 + \rho_1)}. \quad (\text{D. 11})$$

APPENDIX E

VISCOUS DAMPING OF GRAVITY WAVES

The damping of gravity waves by viscosity is treated in Sections 348 and 349 of Lamb. The approximations of Chapter III are similar and clearer than the method employed by Lamb, and for that reason will be used. For stable surface waves in a gravitational field, Eq. (3.45) becomes

$$(n + 2\nu\kappa^2)^2 + \omega_0^2 = 4\nu^2\kappa^3 m \quad (\text{E. 1})$$

where

$$m = (\kappa^2 + n/\nu)^{\frac{1}{2}}. \quad (\text{E. 2})$$

If, for very light damping one assumes

$$n = i\omega_0(1 + \xi), \quad \nu\kappa^2 \ll \omega_0. \quad (\text{E. 3})$$

Equation (E.1) becomes

$$-2\omega_0^2 \xi + 4\nu^2\kappa^4 + 4\nu\kappa^2 i\omega_0 + \omega_0^2 \xi^2 + 4\nu\kappa^2 i\omega_0 \xi \quad (\text{E. 4})$$

$$\approx 4(\nu\kappa^2)^{\frac{3}{4}}(i\omega_0)^{\frac{1}{2}} \left(1 + \frac{\xi}{2} - \frac{i\nu\kappa^2}{2\omega_0}\right).$$

Dividing through by ω_0^2 gives

$$-2\xi + 4\left(\frac{\nu\kappa^2}{\omega_0}\right)^2 + 4i\left(\frac{\nu\kappa^2}{\omega_0}\right) + \xi^2 + 4i\xi\left(\frac{\nu\kappa^2}{\omega_0}\right) \quad (\text{E. 5})$$

$$= 4\left(\frac{\nu\kappa^2}{\omega_0}\right)^{\frac{3}{2}}(i)^{\frac{1}{2}} \left(1 + \xi/2 - i\left(\frac{\nu\kappa^2}{\omega_0}\right)\right).$$

If we drop the terms in $(\frac{\nu\kappa^2}{\omega_0})^{3/2}$, $(\frac{\nu\kappa^2}{\omega_0})^2$, $(\frac{\nu\kappa^2}{\omega_0})\xi$, and ξ^2 , the result is that

$$\xi = 2i \left(\frac{\nu\kappa^2}{\omega_0} \right). \quad (\text{E. 6})$$

So

$$n = i\omega_0 - 2\nu\kappa^2, \quad (\text{E. 7})$$

where the action of $\exp(nt)$ gives damping as $\exp(-2\nu\kappa^2 t)$. For the short wavelength limit, that is, $\nu\kappa^2 \gg \omega_0$, one finds

$$m = (\kappa^2 + n/\nu)^{\frac{1}{2}} \approx \kappa \left(1 + \frac{n}{2\nu\kappa^2} \right). \quad (\text{E. 8})$$

Equation (E. 1) becomes

$$n^2 + 4\nu\kappa^2 n + 4\nu^2 \kappa^4 + \omega_0^2 = 4\nu^2 \kappa^4 (1 + n/2\nu\kappa^2), \quad (\text{E. 9})$$

or

$$n^2 + 2\nu\kappa^2 n + \omega_0^2 = 0. \quad (\text{E. 10})$$

Equation (E. 10) gives

$$n = -\nu\kappa^2 + (\nu^2 \kappa^4 - \omega_0^2)^{\frac{1}{2}}, \quad (\text{E. 11})$$

$$= -\nu\kappa^2 + \nu\kappa^2 \left(1 - \left(\frac{\omega_0}{2\nu\kappa^2} \right)^2 \right)^{\frac{1}{2}}, \quad (\text{E. 12})$$

$$\approx -\nu\kappa^2 + \nu\kappa^2 \left(1 - \frac{1}{2} \left(\frac{\omega_0}{2\nu\kappa^2} \right)^2 \right), \quad (\text{E. 13})$$

$$n \approx -\frac{\omega_0^2}{2\nu\kappa^2}. \quad (\text{E. 14})$$

This is the result for "creeping flow".

APPENDIX F

DERIVATION OF $\omega_0^2 = g\kappa(\rho_2 - \rho_1)/[\rho_2 + \rho_1 \coth \kappa h]$

1. Fixed Upper Surface

Following Lamb (Hydrodynamics, § 231), we take

$$\rho = \rho_1, \quad 0 < y < h, \quad (\text{F. 1})$$

$$\rho = \rho_2, \quad y < 0, \quad (\text{F. 2})$$

and

$$\rho_1 < \rho_2. \quad (\text{F. 3})$$

We require that the velocity in the +y direction vanish at $y = h$. It is assumed that

$$\varphi_1 = A_1 \cosh \kappa(y-h) \cos \kappa x e^{i\omega_0 t}, \quad (\text{F. 4})$$

$$\varphi_2 = A_2 e^{\kappa y} \cos \kappa x e^{i\omega_0 t}, \quad (\text{F. 5})$$

and

$$\eta = a e^{i\omega_0 t} \cos \kappa x. \quad (\text{F. 6})$$

From the definition of η , we find that

$$\frac{\partial \eta}{\partial t} = - \left. \frac{\partial \varphi_1}{\partial y} \right|_{y=0} = - \left. \frac{\partial \varphi_2}{\partial y} \right|_{y=0}, \quad (\text{F. 7})$$

which yields

$$i\omega_0 a = A_1 \kappa \sinh \kappa h = -\kappa A_2. \quad (\text{F. 8})$$

By requiring a continuity of pressure, we find

$$\rho_1(i\omega_0 A_1 \cos \kappa h - ga) = \rho_2(i\omega_0 A_2 - ga). \quad (\text{F. 9})$$

The elimination of A_1 and A_2 from (F. 8) and (F. 9) gives

$$\omega_0^2 = \frac{(\rho_2 - \rho_1)g\kappa}{\rho_1 \coth \kappa h + \rho_2}. \quad (\text{F. 10})$$

2. Free Upper Surface

When the upper surface of the fluid is free, we assume a solution of the form

$$\varphi_1 = (A_1 \cosh \kappa y + B_1 \sinh \kappa y) e^{i\omega_0 t} \cos \kappa x, \quad (\text{F. 11})$$

$$\varphi_2 = A_2 e^{\kappa y} e^{i\omega_0 t} \cos \kappa x, \quad (\text{F. 12})$$

and

$$\eta = a e^{i\omega_0 t} \cos \kappa x. \quad (\text{F. 13})$$

Substitution of these values into (F. 7) gives

$$i\omega_0 a = -\kappa B_1 = -\kappa A_2. \quad (\text{F. 14})$$

The condition of continuity of pressure at the interface gives

$$\rho_1(i\omega_0 A_1 - ga) = \rho_2(i\omega_0 A_2 - ga). \quad (\text{F. 15})$$

At the free surface the requirement is

$$\frac{\partial \eta^*}{\partial t} = - \left. \frac{\partial \varphi_1}{\partial y} \right|_{y=h}, \quad (\text{F. 16})$$

and that

$$\frac{P_1}{\rho_1} = \frac{\partial \varphi_1}{\partial t} - g\eta^* = 0. \quad (\text{F. 17})$$

From (F. 17) we find

$$\eta^* = \frac{1}{g} \left. \frac{\partial \varphi_1}{\partial t} \right|_{y=h}. \quad (\text{F. 18})$$

Applying this result to (F. 16), we find

$$-\frac{\partial \varphi_1}{\partial y} = \frac{1}{g} \frac{\partial^2 \varphi_1}{\partial t^2} \quad \text{at } y=h. \quad (\text{F. 19})$$

This result simplifies to

$$\omega_0^2 \varphi_1 = g \frac{\partial \varphi_1}{\partial y} \quad \text{at } y=h. \quad (\text{F. 20})$$

Substitution of (F. 11) into (F. 20) gives

$$\omega_0^2 (A_1 \cosh \kappa h + B_1 \sinh \kappa h) = g\kappa (A_1 \sinh \kappa h + B_1 \cosh \kappa h). \quad (\text{F. 21})$$

From this we find that

$$A_1 = \frac{\omega_0^2 \sinh \kappa h - g\kappa \cosh \kappa h}{g\kappa \sinh \kappa h - \omega_0^2 \cosh \kappa h} B_1. \quad (\text{F. 22})$$

When the results of (F. 14) are applied, one finds

$$A_1 = \frac{-\omega_0^2 \sinh \kappa h + g\kappa \cosh \kappa h}{g\kappa \sinh \kappa h - \omega_0^2 \cosh \kappa h} \frac{i\omega_0 a}{\kappa}. \quad (\text{F. 23})$$

This result is used in (F. 15) to give

$$\rho_1 \left[\frac{-\omega_o^2}{\kappa} \left(\frac{-\omega_o^2 \sinh \kappa h + g\kappa \cosh \kappa h}{-\omega_o^2 \cosh \kappa h + g\kappa \sinh \kappa h} \right) - g \right] = \rho_2 \left[\frac{\omega_o^2}{\kappa} - g \right], \quad (\text{F. 24})$$

which gives

$$\omega_o^4 (\rho_1 + \rho_2 \coth \kappa h) - \omega_o^2 \rho_2 (1 + \coth \kappa h)g\kappa + g^2 \kappa^2 (\rho_2 - \rho_1) = 0. \quad (\text{F. 25})$$

One root of this equation is

$$\omega_o^2 = g\kappa. \quad (\text{F. 26})$$

This root is not of interest because it describes the case in which both fluids oscillate together. This is just the wave on the free surface.

The other root is

$$\omega_o^2 = \frac{(\rho_2 - \rho_1)g\kappa}{\rho_1 + \rho_2 \coth \kappa h} \quad (\text{F. 27})$$

which is the desired result.

REFERENCES

1. Bellman, R. and Pennington, R. H. , "Effects of Surface Tension and Viscosity on Taylor Instability," *Quart. J. Appl. Math.* , 12, 151, (1954).
2. Chandrasekhar, S. , "The Character of the Equilibrium of an Incompressible Heavy Viscous Fluid of Variable Density," *Proc. Phil. Soc.* , 51, 162, (1955; see also Chandrasekhar, S. , Hydrodynamic and Hydromagnetic Stability, (Oxford, 1961), Chap. X.).
3. Lamb, H. , Hydrodynamics, 6th ed. (Dover, 1945), 623-25.
4. Rayleigh, Lord, "Investigation of the Character of the Equilibrium of an Incompressible Heavy Fluid of Variable Density," *Proc. Lond. Math. Soc.* , 14, 170, (1883).
5. Taylor, G. I. , "The Instability of Liquid Surfaces when Accelerated in a Direction Perpendicular to Their Planes. I," *Proc. Roy. Soc. A*, 201, 192 (1950).
6. Lamb, H. , op. cit. , 370-72.
7. Lamb, H. , op. cit. , 456-57.
8. Harrison, W. , "The Influence of Viscosity on the Oscillations of Superposed Fluids," *Proc. Lond. Math. Soc.* 6, 396, (1908).
9. Plesset, M. S. , and Whipple, C. G. , "Viscous Effects in Rayleigh-Taylor Instability," *Phys. Fluids*, 17, 1, (1974).
10. Lewis, D. J. , "The Instability of Liquid Surfaces when Accelerated in a Direction Perpendicular to Their Planes. II," *Proc. Roy. Soc. A*, 202, 81, (1950).
11. Emmons, H. W. , Chang, C. T. , and Watson, B. C. , "Taylor Instability of Finite Surface Waves," *J. Fluid Mech.* , 7, 177, (1960).
12. Cole, R. L. , and Tankin, R. S. , "Experimental Study of Taylor Instability," *Phys. Fluids*, 16, 1810, (1973).
13. Plesset, M. S. and Winet, H. , "Bioconvection: Sedimentation Fingers in Motile Cell Cultures as an Example of Rayleigh-Taylor Instability," *Nature*, in press.
14. Platt, J. R. , "'Bioconvection Patterns' in Cultures of Free-Swimming Organisms," *Science*, 133, 1766, (1961).

15. Winet, H., and Jahn, T. L., "On the Origin of Bioconvective Fluid Instabilities in Tetrahymena Culture Systems," Biorheol., 9, 87, (1972).
16. Happel, J., and Brenner, H., "Low Reynolds Number Hydrodynamics," (Prentice-Hall, 1965), 384.
17. Happel, J., and Brenner, H., op. cit., 156.

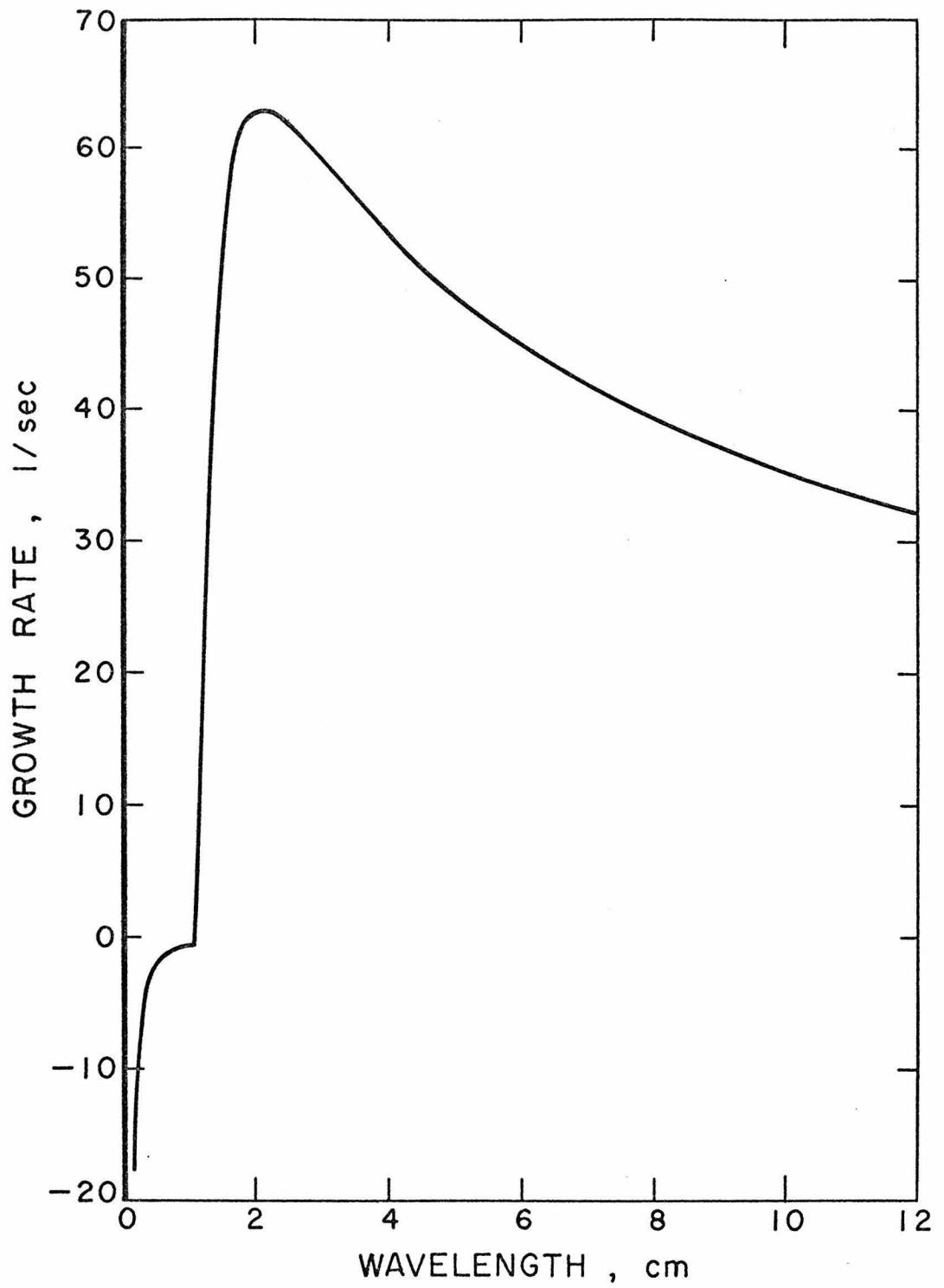


Fig. 4 Growth rate versus wavelength for water accelerated into air.

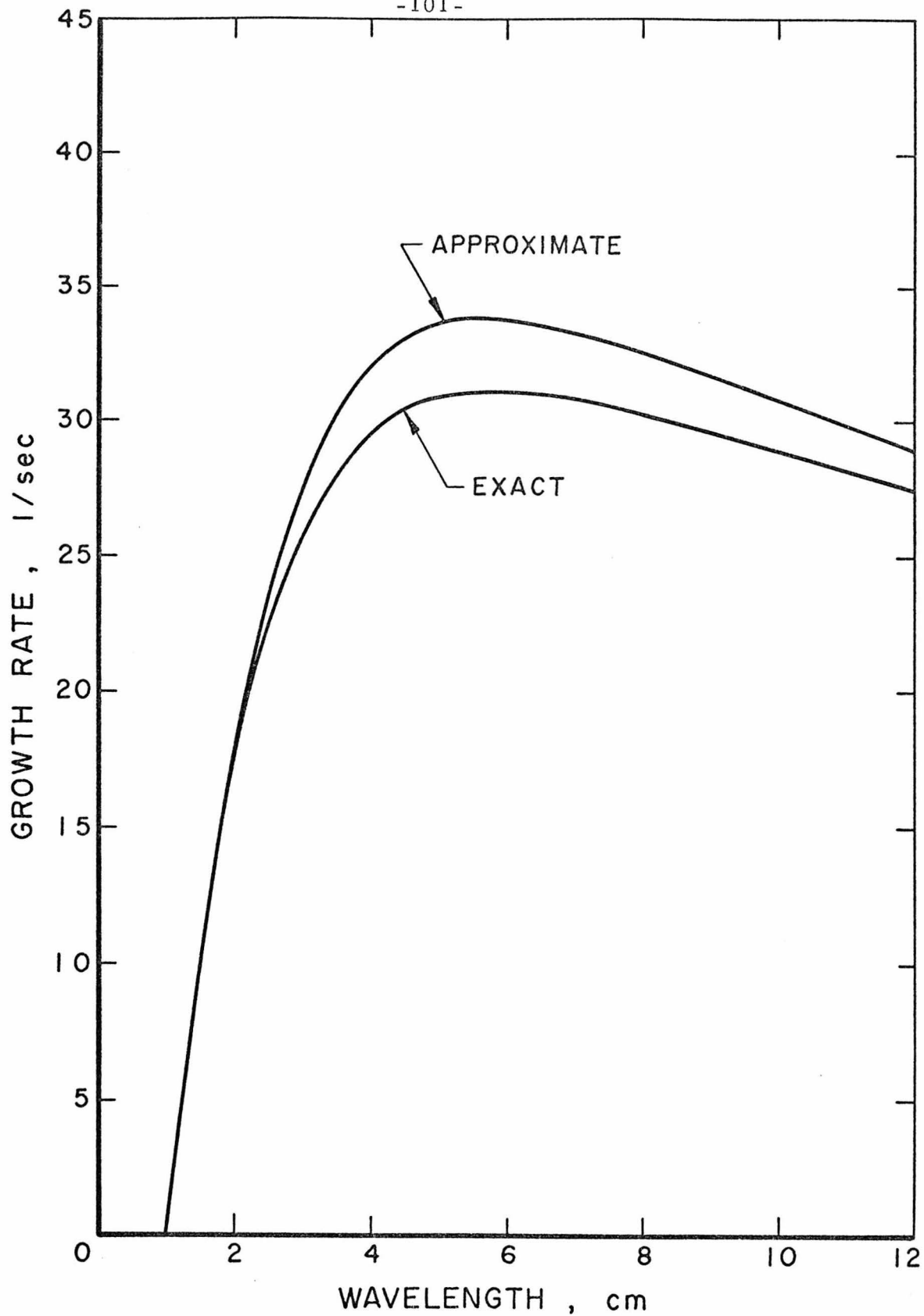


Fig. 5 Growth rate versus wavelength for glycerol accelerated into air.

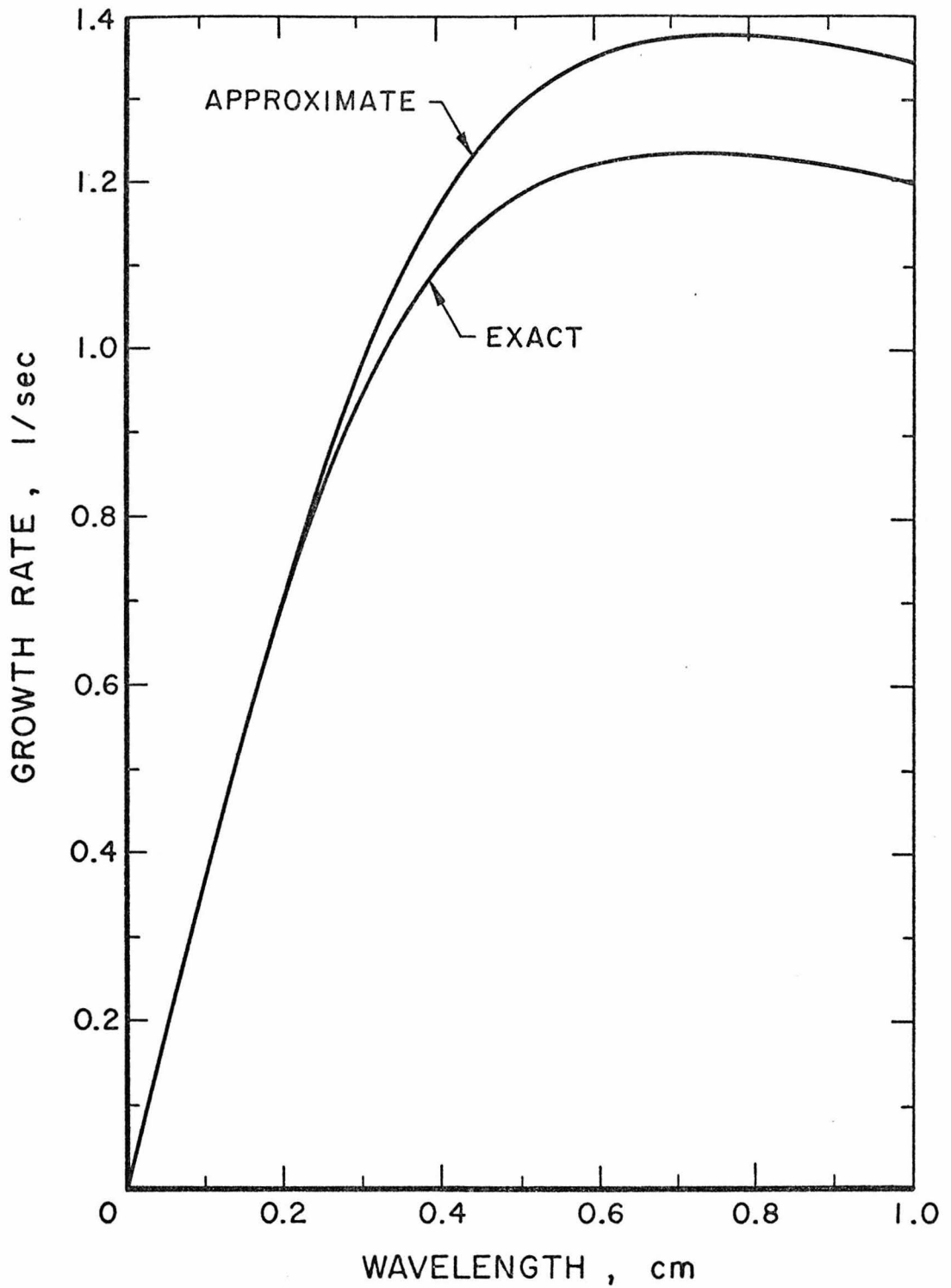


Fig. 6 Growth rate versus wavelength for the small density difference case; $\Delta\rho = 9.42 \times 10^{-4}$.

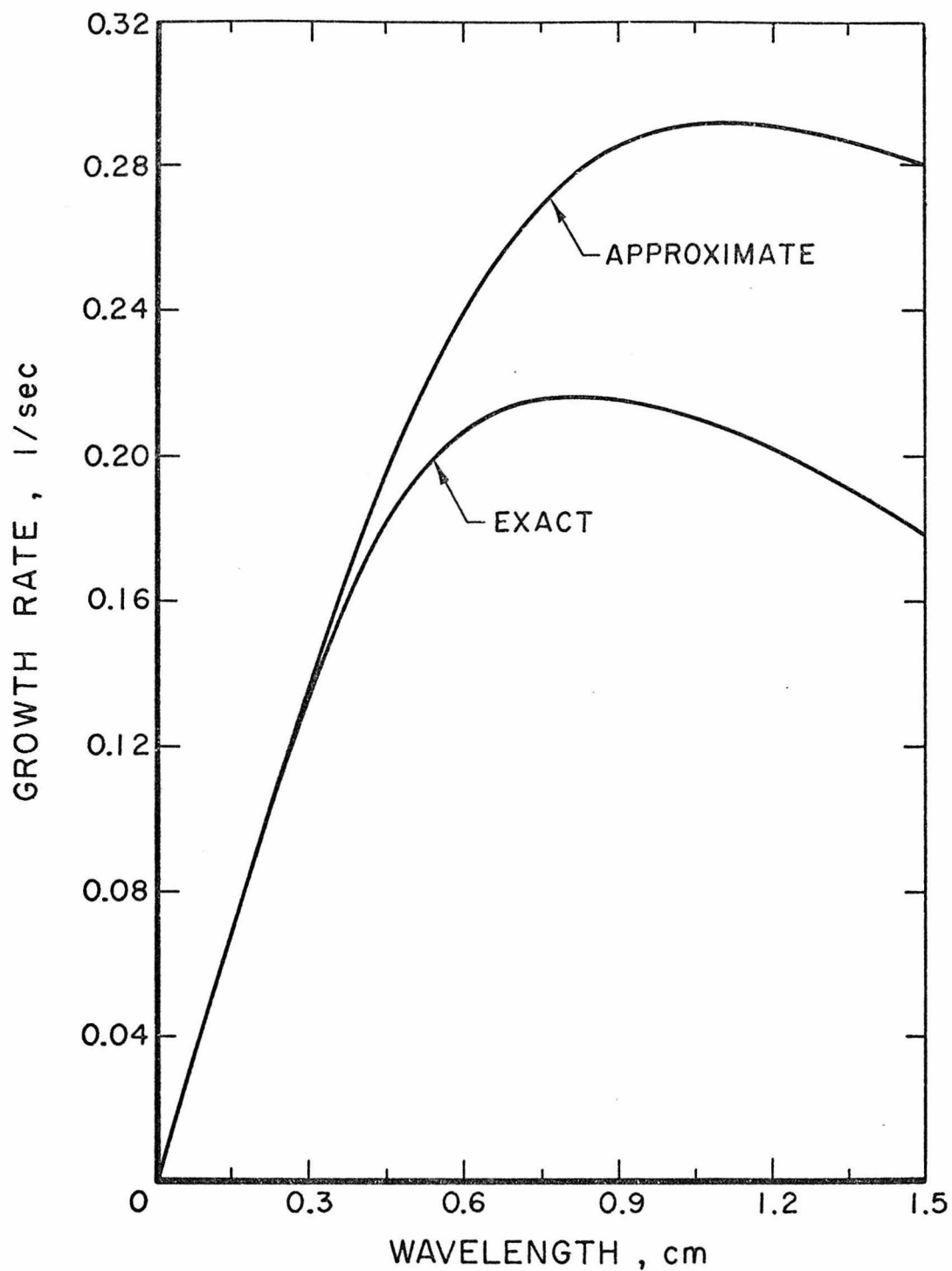


Fig. 7 Growth rate versus wavelength for the small density difference case with a free surface at $y = h$; $\Delta \rho = 1.21 \times 10^{-4}$.

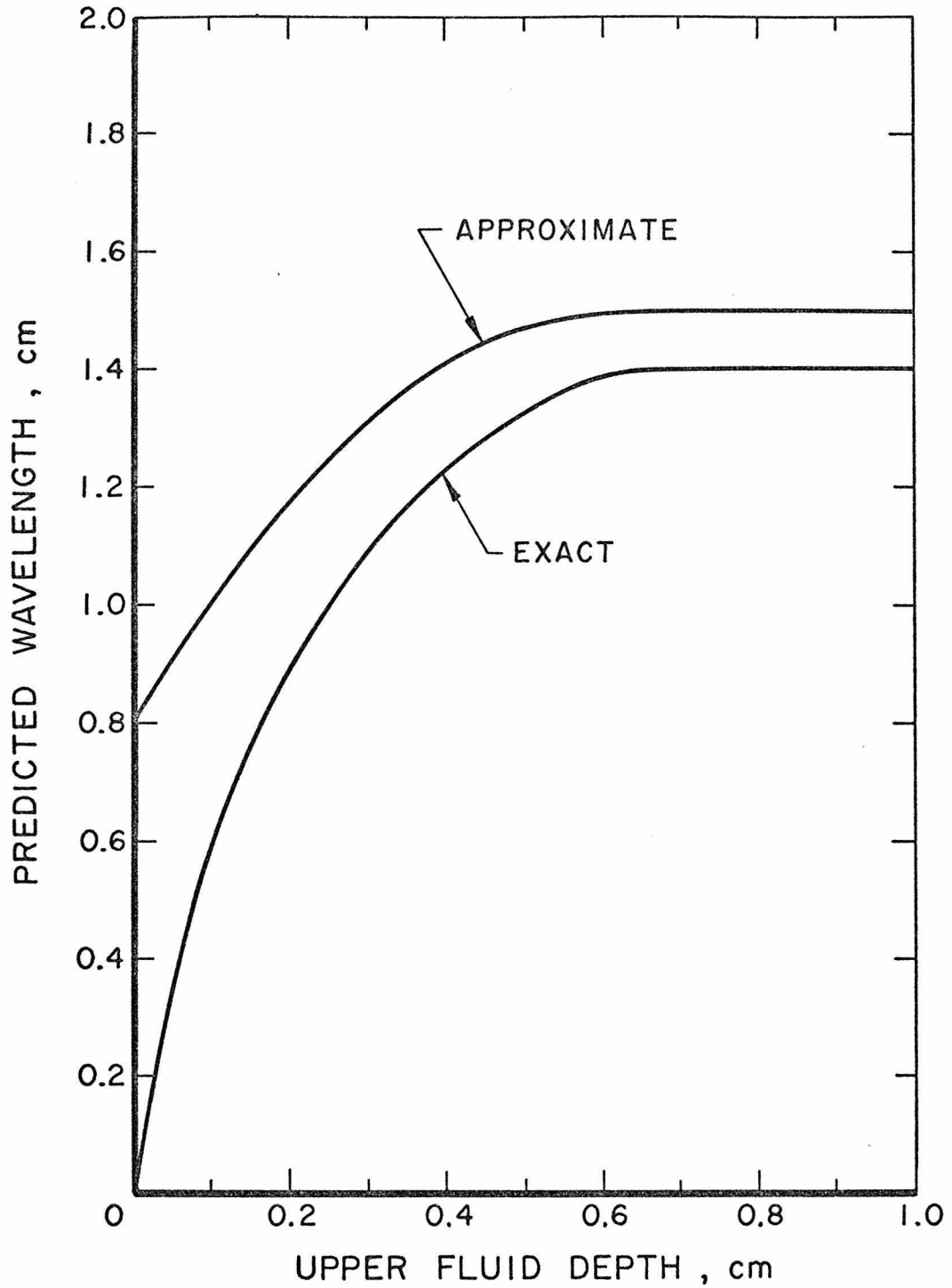


Fig. 8 Preferred wavelength versus depth for small density difference, free surface case; $\Delta \rho = 1.21 \times 10^{-4}$.

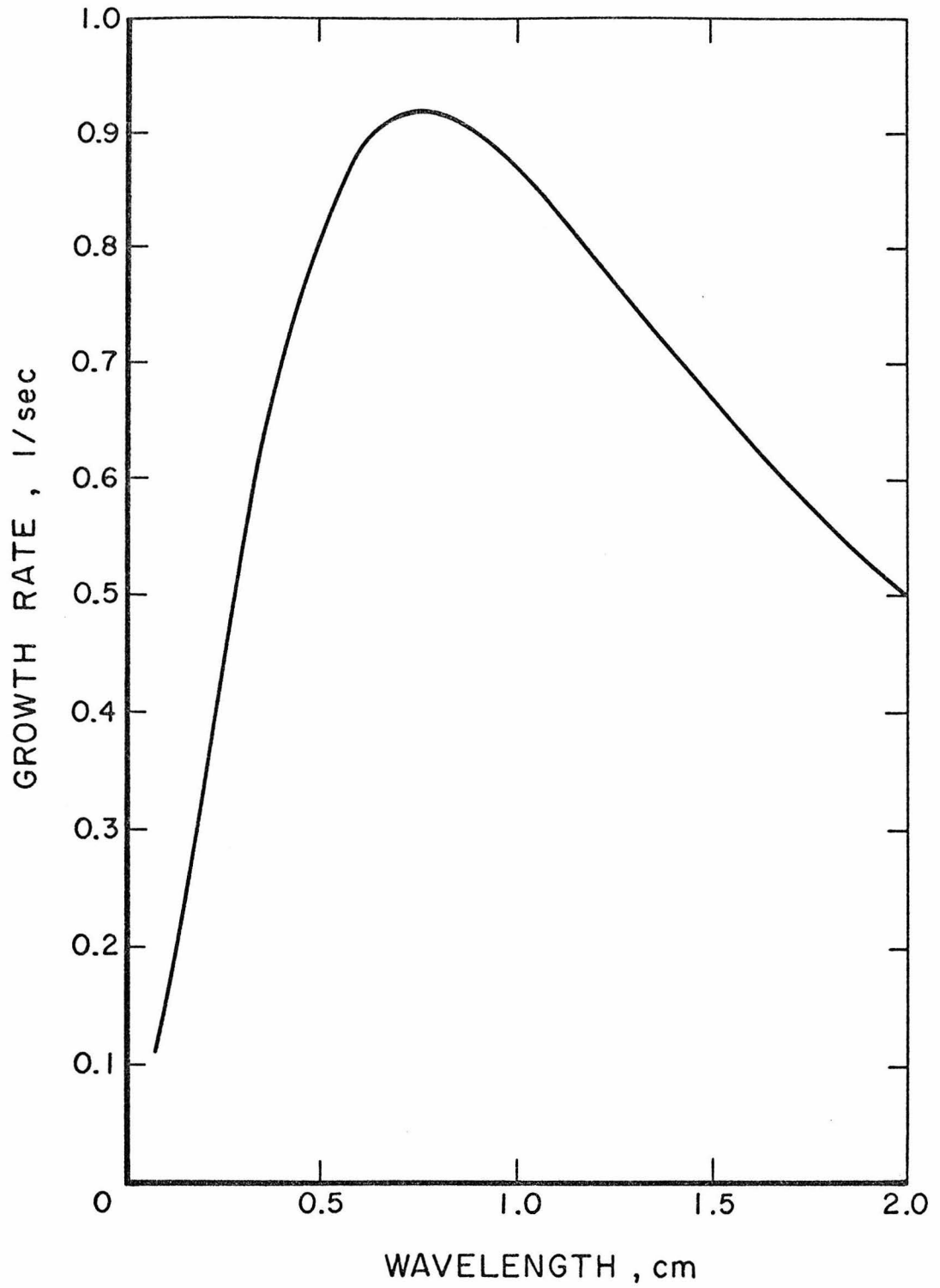


Fig. 9 Growth rate versus wavelength for rigid upper boundary.

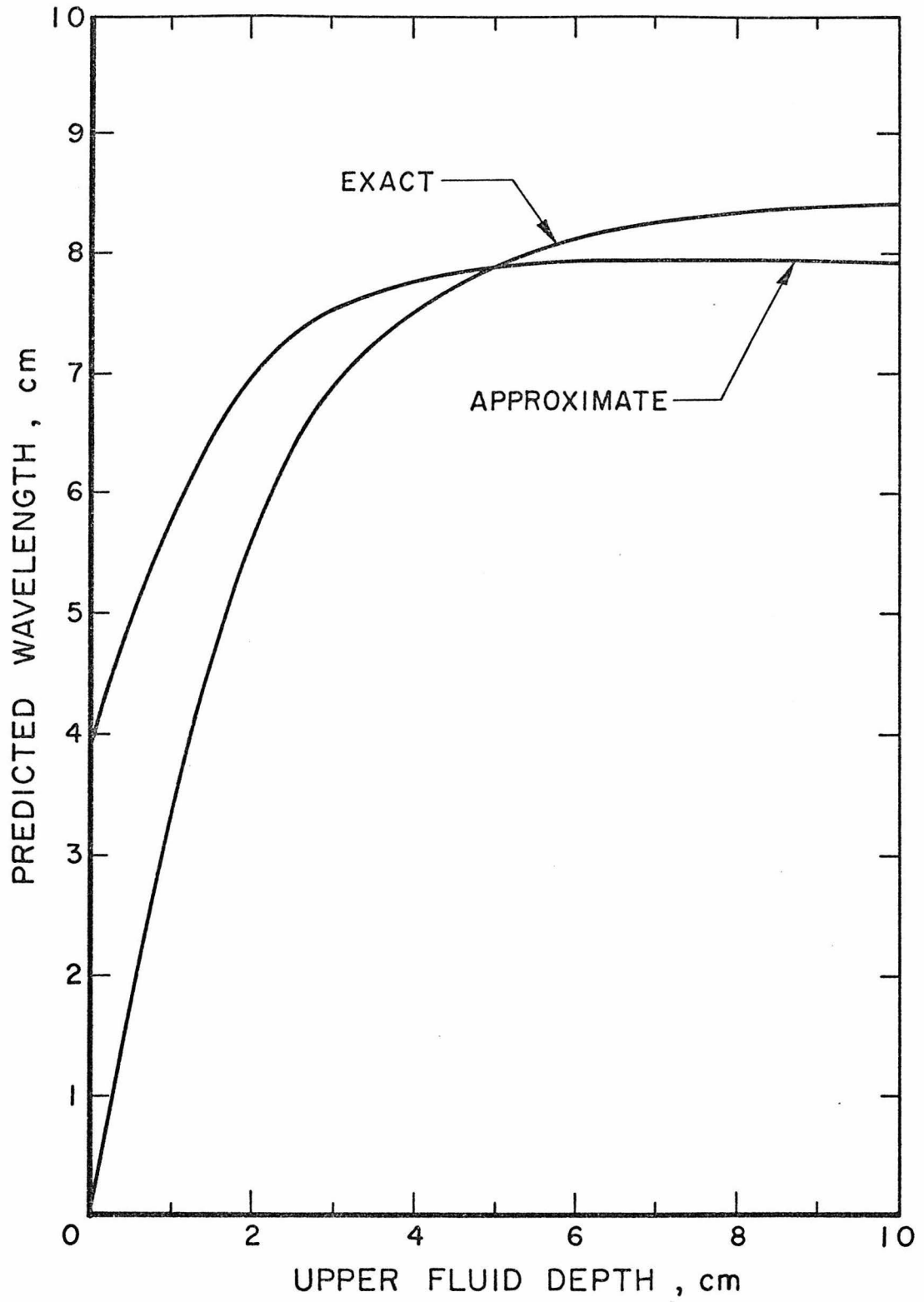


Fig. 10 Preferred wavelength versus depth for rigid boundary case.

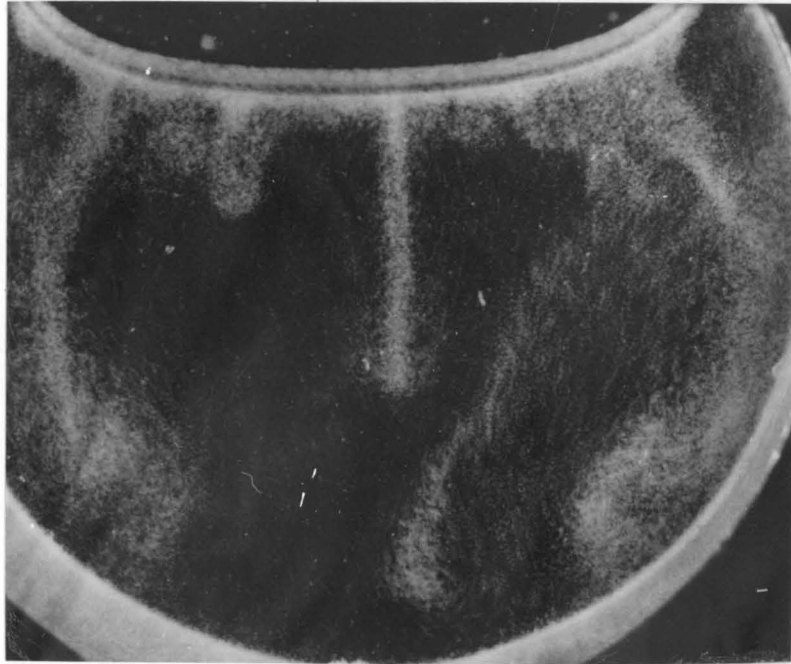


Fig. 11 Side view of Tetrahymena pyriformis culture.

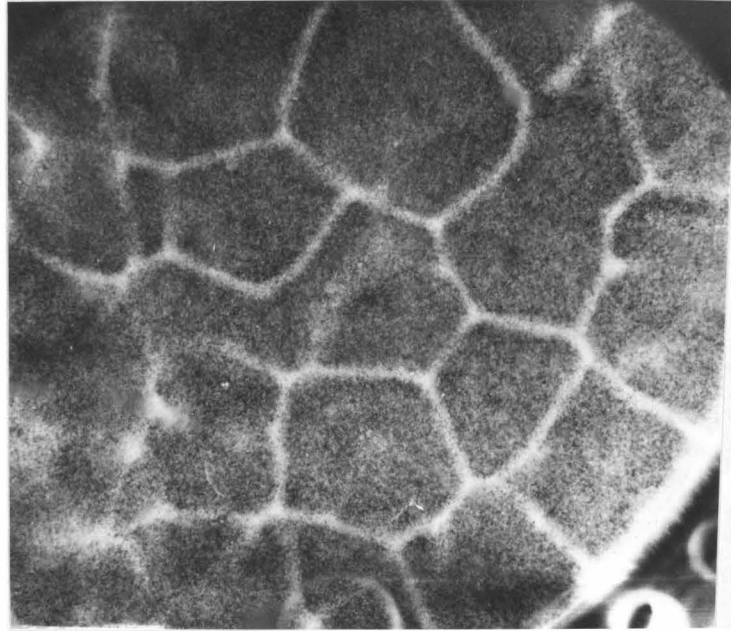


Fig. 12 Top view of Tetrahymena pyriformis culture.

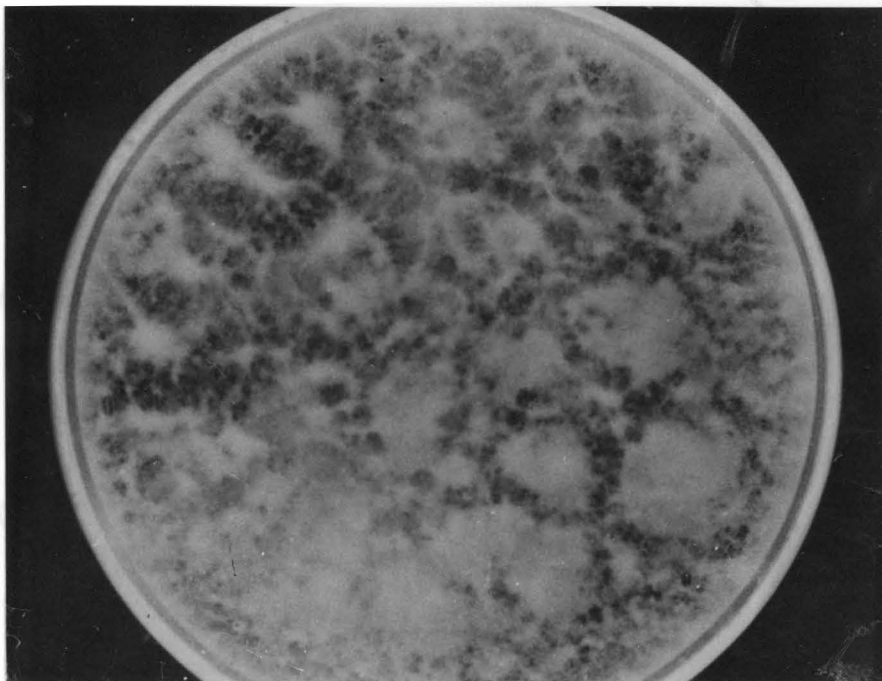


Fig. 13 Top view of glass beads in viscous liquid.

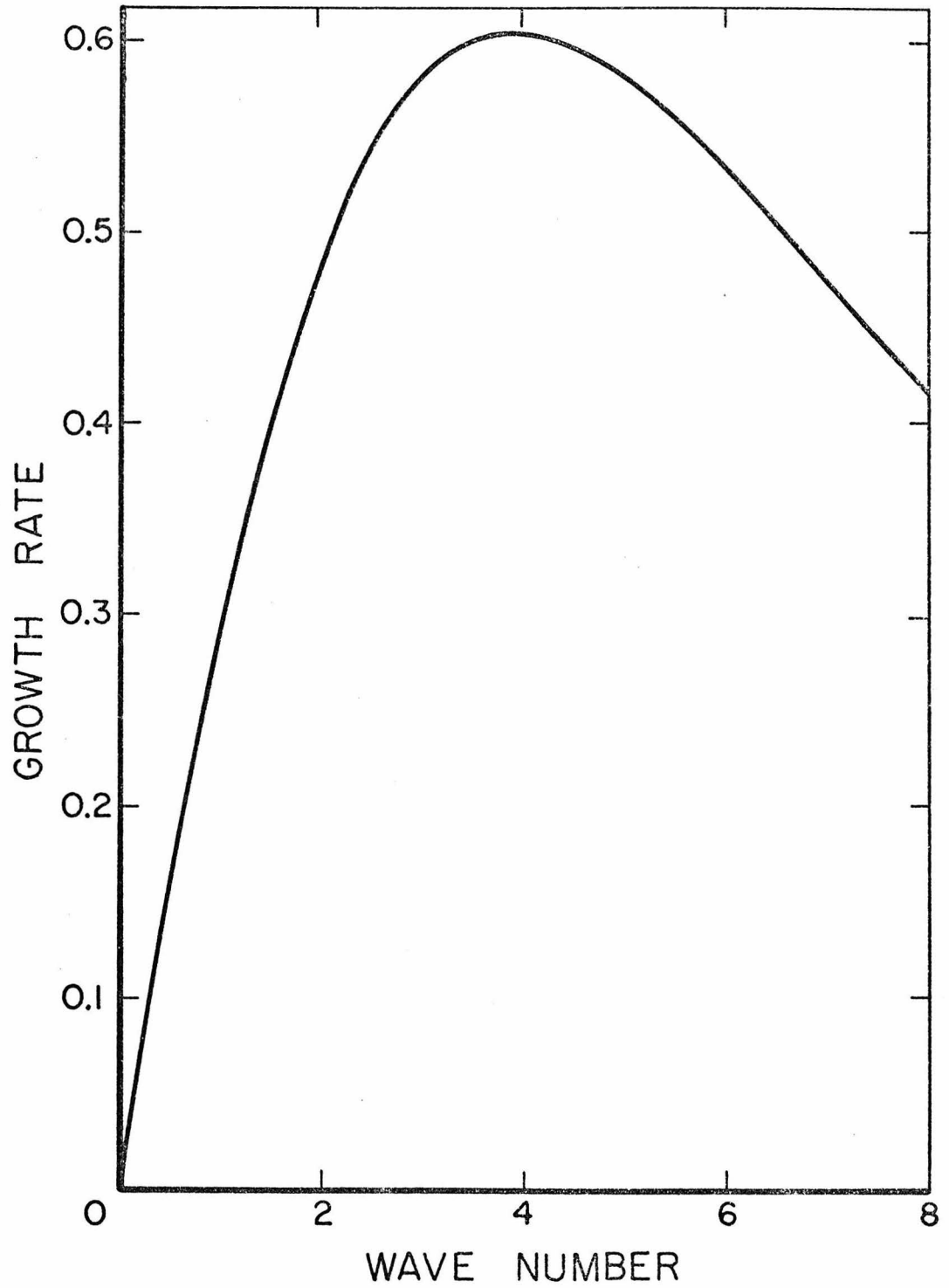


Fig. 14 Nondimensional curve of growth rate versus wave number for exponential density gradient.